University of South-Eastern Norway

www.usn.no

FMH606 Master's Thesis 2022

Master of Science, Process Technology

Utilization of captured CO_2: Enhanced esterification reactions using membrane reactor

Edirisinghe Arachchige Viraj Udasri Edirisinghe

Faculty of Technology, Natural sciences and Maritime Sciences

Campus Porsgrunn

University of South-Eastern Norway

www.usn.no

Course: FMH606 Master's Thesis, 2022

Title: Utilization of captured CO_2: Enhanced esterification reactions using membrane reactor

Number of pages: 73

Keywords: pervaporation, esterification, membranes

Student: Edirisinghe Arachchige Viraj Udasri Edirisinghe

Supervisor: Klaus-Joachim Jens

External partner: -

Summary:

About 80% of worldwide CO_2 emissions are from large stationary sources that need to be lowered to reduce the impact on the environment. One step towards this goal is to capture CO_2 from post-combustion and use it as a feedstock for ester production. It is possible to improve the ester product by shifting the equilibrium reaction by removing water from pervaporation.

The purpose of this study was to construct an experimental setup to test a model esterification reaction and make recommendations for a future NFR-funded project. However, due to complications, ethanol-water mixture was used to study the membrane separation of the pervaporation reactor.

Experiments were done for varying initial compositions as well as varying temperatures. The results showed the experimental setup works as expected and promising separation could be achieved for PERVAP^{TM} 4100 membrane. With further modifications to the experimental setup, a more complete pervaporation reactor setup could be built.

Preface

This task was provided by the University of South-Eastern Norway for the subject FMH606 Master's Thesis, spring 2022. The task is supplementary to the newly funded project ALCOPOP (ALCOhol-based PrOcess for Production of carbonic acid diesters from CO_2) by The Research Council of Norway.

The Master's Thesis project supervisors consisted of main supervisor Professor Klaus-Joachim Jens, Professor Marianne Eikeland and Associate professor Zulkifli Idris from USN.

I am grateful to Professor Klaus-Joachim Jens for always providing insightful comments, as well as taking the time to help and guide throughout the project despite his hectic schedule. Secondly, I would like to thank Professor Marianne Eikeland for helping me to expand my knowledge of membrane technology and for providing a membrane cell and testing membranes for the experiment. I would also like to express gratitude to Associate professor Zulkifli Idris for his assistance during the initial planning stages as well as for providing valuable supplies and tools during the experimental setup construction. In addition, I would like to acknowledge Jayangi Dinesha Wagaarachchige for helping me to understand Raman spectroscopy and for providing me with insight into the preprocessing of data collected from sample analysis. Further, I would like to express my appreciation to Fredrik Hansen, who provided the necessary feeding pumps with controllers and also helped to create a LabVIEW program to measure flow. Lastly, I would like to thank Eirik Rugstad Haugen and Chidapha Deeraksa for supporting me to locate the equipment needed for this project.

Porsgrunn, 25.05.2022

Edirisinghe Arachchige Viraj Udasri Edirisinghe

Contents

Nomenclature

CA	Cellulose Triacetate
CP	Carbomer
CPVC	Carboxylated Polyvinyl Chloride
DSC	Differential Scanning Calorimetry
DTA	Differential Thermal Analysis
ESCA	Electron Spectroscopy for Chemical Analysis
GC	Gas Chromatography
GCCS	Glutaral Cross-Linked Chitosan
GCHA	Glutaral Crosslinked Gelatin
IR	Infrared
NA	Nafion
NMR	Nuclear Magnetic Resonance Spectroscopy
PAN	Polyacrylonitrile
PDMS	Polydimethylsiloxane
PEBA	Polyetherpolyamide Block-Copolymer
PES	Polyethersulfone
PLS	Partial Least Square
PV	Pervaporation
PVA	Polyvinyl Alcohol
PVC	Polyvinyl Chloride
PVR	Pervaporation Reactor
R	Initial Molar Ratio of Alcohol to Acid

UV	Ultraviolet
XPS	X-Ray Photoelectron Spectroscopy

1 Introduction

The highest amount of greenhouse gas emissions come from carbon dioxide (CO_2) globally. CO_2 emissions can be reduced by capturing CO_2 using a variety of methods and techniques. However, it is worth noting that no global product can capture the vast amount of globally emitted CO_2, and CO_2 as a part of a product will be always returned to the atmosphere sooner or later. The captured CO_2 from emission sources such as post-combustion exhaust gas has a negative value since the producer will have to pay for transport and storage. Therefore, it could become a source of low-cost raw material and utilized to produce valuable products. Among the methods being explored to utilize captured CO_2 is ester formation. Typically, membrane separation can improve ester conversion, and its implementation for ester formation from CO_2 is currently being explored

Chemically, an ester is a compound created when one or more of the hydroxyl groups in an acid are changed for alkyl groups [1]. It is more common to find ester derived from carboxylic acids. A carboxylic acid and an alcohol are usually reacted in the presence of a catalyst to produce these. The process is called esterification. The esterification reaction between Acetic acid and Ethanol is an example.

Because of its characteristic pleasant smell, esters are used in flagrant production and can also be found in essential oils. Natural esters can be extracted from plants, but they are often limited by their high operational costs, occasional shortages in supply, and regional differences in quality and quantity of flavor [2]. It is in this circumstance that the production of esters by a suitable technique has attracted researchers and entrepreneurs.

1.1 Background

About 80% of the worldwide CO_2 emissions from large stationary sources, originate from flue gas from power stations [3] and using CO_2 capture units, it is possible to capture CO_2 from flue gas streams. ‘ALCOhol-based PrOcess for Production of carbonic acid diesters from CO_2 (ALCOPOP)’ is a newly funded project by The Research Council of Norway that focuses on finding a new process concept for the synthesis of ethylene carbonate from CO_2 and biomass sourced ethylene glycol via amine pre-activation of CO_2. Using CO_2 captured by the capture unit as feedstock, the project will aim to enhance carbonate ester yield and reduce the energy needed to capture CO_2. Water formation during carbonate production from CO_2 is a limitation to the forward reaction of the equilibrium [4]. Therefore, to remove water from such system should be studied.

As a thermodynamic and equilibrium-limited reaction, esterification reactions often have limited product conversion and low purity [5]. Multiple methods can be used to intensify the reaction by shifting equilibrium towards the ester formation. Chemical reactions combined with distillation separation are used in reactive distillation, which removes a product from a reaction medium [6]. In some of the ester production processes that use this method, a large amount of alcohol is used, hence increasing the cost of the equipment [7]. In addition, the high-boiling ester separation requires a higher temperature, consequently increasing the operating costs [8].

Pervaporation is another hybrid process that combines chemical reaction with membrane separation for removing a product. Recent attention has been paid to pervaporation in the

chemical industry due to high selective separation and low energy consumption [9, 10]. Pervaporation is attractive for esterification since membrane separation relies on the solubility and diffusivity of components to transport components through a membrane, whereas reactive distillation relies on the relative volatility of components, an approach that encounters limitations.

1.2 Objectives

This project aims to observe the ethyl acetate synthesis esterification reaction as a model equilibrium reaction. Removal of the by-product, water, would increase the rate of the forward reaction and improve the ester formation. A membrane separator will be setup to remove water from the system and water separation will be studied. Once the experimental setup has been completed, a series of experiments will be conducted to observe the effects of the different operating conditions and test the performance of suitable membranes. Several tasks will be carried out to accomplish this:

I. Literature study on esterification reaction, pervaporation (membrane) technology.
II. Setting up the membrane reactor with help from supervisors and fit for purpose test.
III. Testing of esterification reactions and study of different membranes.
IV. Discussion/recommendation on improvement to the system.

Even though the objectives were set as mentioned above, complications arose due to unavailability of analytical techniques for the samples and unexpected time consumption for the construction of the experimental setup. As a result, experiment plans had to be revised accordingly to observe membrane separation of water from water-ethanol liquid mixtures where water separation could be studied.

1.3 Report structure

The report will start with a general introduction to the theoretical knowledge on esterification, pervaporation and the analysis techniques used will be given. After that literature study on esterification reaction utilizing pervaporation (membrane) technology will be presented. Furthermore, experimental setup including construction and testing and the experiments themselves will be presented. Some Results will be given for experiment setup construction and experiments and later discussed in the results and discussion chapter. Finally, conclusions are drawn and some thoughts about further work will be discussed.

2 Theory

The third objective of this project is the testing of esterification reactions and the study of different membranes. Therefore, the knowledge of esterification, membrane separation via pervaporation, and the analytical techniques used to observe results are pre-requisites for the project. Thus, under this chapter, the theoretical background of above-mentioned subtopics will be mainly discussed.

2.1 Esterification chemistry

Esterification is the formation process of ester (R-COO-R) with water, by the combination of an organic acid (R-COOH) with an alcohol (R-OH). This ester formation is an equilibrium reaction, and the behavior varies according to conditions provided. An introduction to esterification, esterification process from acetic acid and ethanol and the important parameters for esterification are discussed below.

2.1.1 Introduction to esterification

As it is mentioned in introduction, when a carboxylic acid reacts with alcohol, esterification occurs. An acid catalyst and heat can increase the rate of reaction. Removing a -OH from the carboxylic acid needs high energy content hence a catalyst and heat are required to provide the required energy. The basic chemical equilibrium reaction is depicted in Figure 2.1.

$$RCOOH + R'OH \rightleftharpoons RCOOR' + H_2O$$

Figure 2.1: Basic esterification reaction [11].

Esterification is a somewhat slow and reversible process. The equilibrium determines the limiting conversion of the reactants.

2.1.2 Esterification of Acetic acid and Ethanol

The esterification process of ethyl alcohol and acetic acid, catalyzed by sulfuric acid, has been studied at various conditions and catalyst dosages.

A batch reactor was utilized to collect operational data, according Atalay et al. [12]. The tests were run with constant beginning ethanol and acetic acid concentrations, and the data were analyzed using a differential analytic approach to determine the sequence of reaction in forward and reverse situations. In the presence of concentrated H_2SO_4, the total esterification process of acetic acid with ethanol is shown in Figure 2.2.

Figure 2.2: Ethyl acetate production from acetic acid and ethanol.

Earlier investigations of the esterification reaction between ethyl alcohol and acetic acid thought it was second order for both forward and reverse reactions [13, 14]. However, Otera and Nishikido [11] experimentally demonstrated that the orders of forward and reverse reactions were 1 and 2, respectively.

Beula et al. [15] investigated the esterification of acetic acid and ethanol in an isothermal batch reactor using a homogenous acid catalyst sulfuric acid. The reaction's progress was tracked by measuring the concentration of water with a Karl Fischer titrator. The reactant mole ratio, reaction temperature, and catalyst concentration are all factors. The processing conditions for increased ester production were determined. To determine the order of the reaction, the experimental data were analyzed using an integral technique.

Beula et al. [15] discovered that at a constant molar ratio, catalytic concentration, and temperature rise, there was no significant improvement in conversion. However, the time required to achieve the equilibrium conversion was dramatically lowered. The same outcome was obtained when the catalyst concentration was raised as with the temperature impact. However, when the molar ratio was raised, the conversion of ethyl acetate increased due to the presence of surplus alcohol. Beula et al. [15] also demonstrated that the reaction is second order in both forward and reverse orientations, and the kinetic parameters were calculated using this model.

Therefore, it is quite evident after exploring the results of above-mentioned studies that the order of the reaction forward and reverse reaction is same which is 2. Moreover, initial mole ratio of reactants, operating temperature and catalyst composition are the three major parameters that governs the chemical kinetics of the esterification reaction between ethyl alcohol and acetic acid.

2.2 Pervaporation technology

Membrane separation is a separation technology used to separate components in a fluid, with the use of selective barrier called “membrane”. To separate components within a stream, certain components are allowed to pass (permeate) through the membrane, while other components are retarded (retentate) from passing through [16].

The concept of pervaporation is based on the combination of permeation and evaporation in order to make membrane separation more energy efficient [16]. The pervaporation process can remove volatile compounds from solutions through the use of a selective membrane. The volatile compounds dissolved in liquids diffuse through dense membranes when a vacuum or purge gas is created on one side. The appropriate selection of membrane according to requirement is based on many factors [16].

In this section the materials used to produce membranes, membrane types and characterization and an introduction to the pervaporation will be given.

2.2.1 Membrane materials

Normally materials used to form membranes can be classified into two main categories according to the type of material, as biological membranes, and synthetic membranes [16] as shown in the Figure 2.3. All living cells are surrounded by biological membranes, but they differ fundamentally from synthesized organic and inorganic membranes in structure and function. The different types of membrane materials used in synthetic membranes may be further subdivided into organic (polymeric) and inorganic membranes, with organic membrane materials being the most commonly used. The selection of polymer as a membrane material depends on the specific properties such as, thermal, chemical, and mechanical properties of polymers and permeability, which are determined basically by structural factors [16].

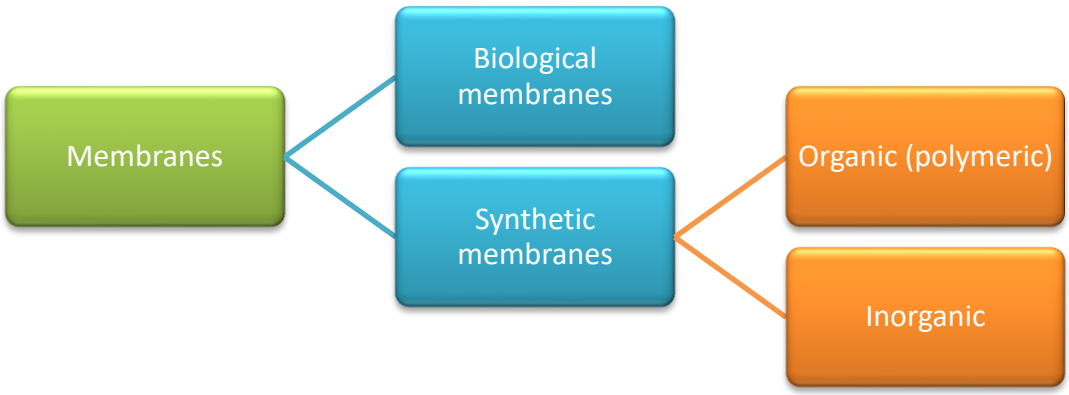

Figure 2.3: Membrane classification according to the type of material used.

A polymer is composed of a large number of monomers, each of which has a very high molecular weight. The degree of polymerization of a molecule is measured by the number of structural units that are linked together to form it. The following Table 2.1 shows some structural parameters affecting the properties of polymer membranes [16].

Table 2.1: Structural parameters affecting the properties of polymer membranes.

Structural parameters	Description
Molecular weight	An organic molecule's molecular weight is determined by the degree of polymerization and by the molecular weight of its fundamental unit, the monomer.
Chain flexibility	Flexibility of the chain is determined by the type of main chain and the presence and nature of its side chains. A typical main chain is composed solely of C-C bonds, and these bonds are capable of being rotated, which makes it more flexible. The main chain is impossible

	to rotate since it contains only C=C bonds (unsaturated), resulting in an extremely rigid structure. The presence of aromatic or heterocyclic groups in the main chain results in a significant loss of flexibility. Oxygen and nitrogen are generally found in a main chain linked to a carbon atom, thus increasing the degree of flexibility.
Chain interactions	Dispersion forces (or London forces) are the most common forces that can induce chain interactions. Bonding forces between hydrogen molecules are the strongest secondary forces
State of the polymer	The phase in which a polymer appears is defined as 'the state of the polymer'. This is a more complex polymer than low molecular weight compounds. As an example, there could be a rubbery solid phase or a glassy solid phase, but the properties would differ widely.

The general rule is that any polymer could be used as a barrier or membrane. However, due to their varying chemical and physical properties, only a limited number could be used practically.

Membranes made of polymeric materials can also be categorized as open porous and dense non-porous, according to different application requirements in membrane separation [16].

2.2.1.1 Open porous membranes

Microfiltration and ultrafiltration are usually performed using open porous membranes [16]. The open porous membrane is selected based on the process requirements, fouling characteristics, and thermal and chemical stability. A significant challenge in ultrafiltration/microfiltration is the decline in flux as a result of concentration polarization and fouling. Consequently, the choice of material should be based on preventing fouling and cleaning membranes after fouling. Similarly, if the polymeric material is intended for use in non-aqueous solutions or at high temperatures, chemical and thermal resistance are important characteristics [16].

2.2.1.2 Dense non-porous membranes

In pervaporation and gas separation, dense nonporous membranes are applied [16]. The membranes used in these applications are either composite membranes or asymmetric membranes. The intrinsic properties of the membrane material can be used to figure out its permeability and selectivity.

2.2.1.3 Characterization of nonporous membranes

For molecular separations, nonporous membranes are used [16]. Basically, transport through non-porous membranes happens due to the solution-diffusion mechanism, and separation occurs due to differences in solubility and diffusivity. Therefore, such membranes cannot be identified by methods that determine pore size or pore size distribution. Because of that, it is

more important to determine the physical properties of chemical structures in membranes. The following Table 2.2 represent the methods used to determine those properties [16].

Table 2.2: Different nonporous membrane characterization methods.

Nonporous membrane characterization method	Description
Permeability measurement	The most direct and simplest way to characterize a nonporous membrane is to determine its permeability towards liquids and gases. Glass transition temperatures (T_g) and crystallinity are the two main parameters that influence membrane permeability. Glassy polymers are generally less permeable than elastomers. Depending on the glass transition temperature, a polymer is either glassy or rubbery. There are several factors that can affect the permeability coefficient, including test conditions and type of gas used. The crystallinity can be determined by different methods such as DSC and DTA, X-ray diffraction, and by spectroscopy (IR and NMR).
Plasma etching	This is a new technique that is used to measure the thickness of the top layer in asymmetric and composite membranes. Additionally, it is possible to determine the structure of the top layer and the properties of the layer immediately below the top layer.
Surface analysis method	In surface analysis methods, an excitation of a solid surface occurs by means of radiation or particle bombardment. This technique provides information regarding the presence of specific groups, atoms, or bonds. Some of surface analysis methods are X-ray Photoelectron Spectroscopy (XPS and Electron Spectroscopy for Chemical Analysis (ESCA).

Thus, the nonporous membranes which are mainly used for pervaporation can be characterized and selectively used for many industrial applications.

2.2.2 Pervaporation

The principle of pervaporation is the separation of liquid mixtures by partial vaporization mainly through a nonporous membrane. Permeating components in vapor form are then collected, which may be removed by flowing an inert medium (sweep gas) or by applying low pressure to the permeating side [17] as shown in Figure 2.4. An important factor in the

pervaporation process is the difference in chemical potential, which is a function of the concentration gradient between the phases on either side of the barrier.

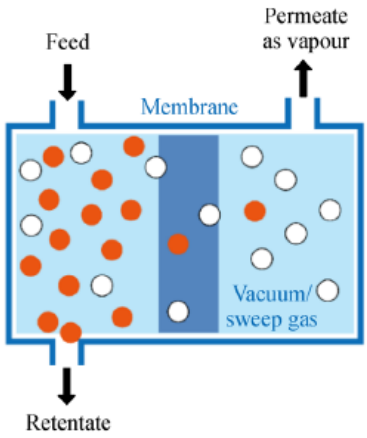

Figure 2.4: Schematic of pervaporation process [17].

As an industrial application, esterification is a typical example of utilizing the pervaporation membrane reactor in the hybrid configuration to remove the products or byproducts of a reaction. The esterification is usually known as a reversible process resulting in water and an ester as the end products. In pervaporation membrane reactors (PVR) the water is removed selectively through a membrane in order to increase the ester production yield.

2.2.2.1 Mass transfer mechanism in pervaporation

The mass transfer mechanism through the membrane, depends on the membrane material and the type of components (feed) which is subjected to separate as shown in Figure 2.5.

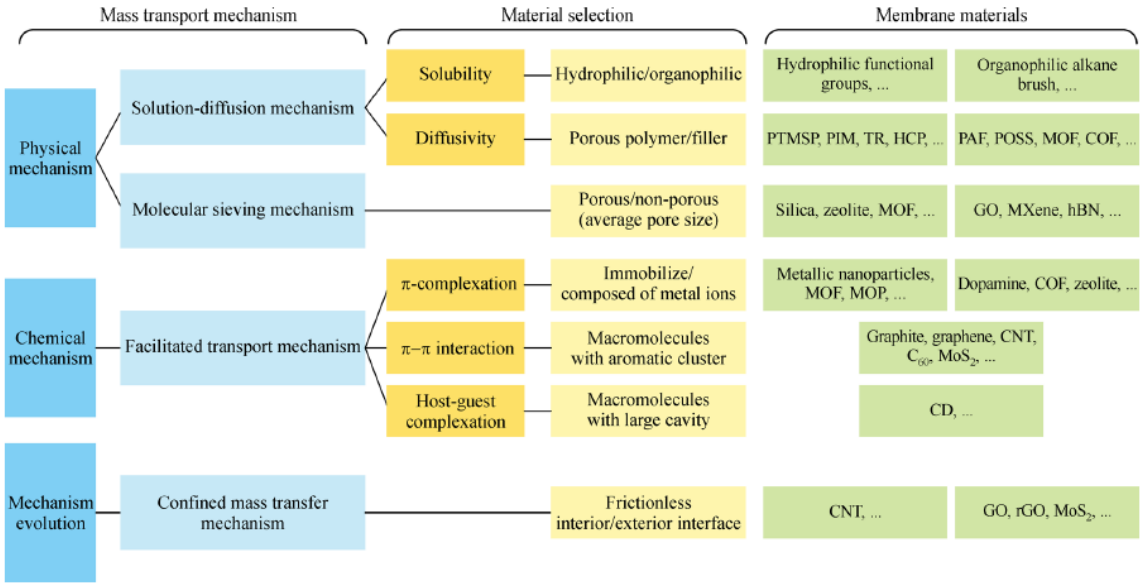

Figure 2.5: Membrane materials that derive from different mass transport mechanisms [17].

The membrane used in this project is polyvinyl alcohol (PVA) hydrophilic membrane and it belongs to the category of materials with hydrophilic functional groups. Therefore, according to the Figure 2.5 it can be assumed that the main mass transfer mechanism in pervaporation is the physical solution-diffusion mechanism.

The solution-diffusion mechanism is the result of these processes in series (Figure 2.6):

1. The diffusion of the component to the membrane surface through the liquid boundary layer.
2. Diffusion or sorption to the membrane.
3. Transportation through the membrane.
4. Diffusion transport into the bulk of the permeance through the vapor phase boundary layer.

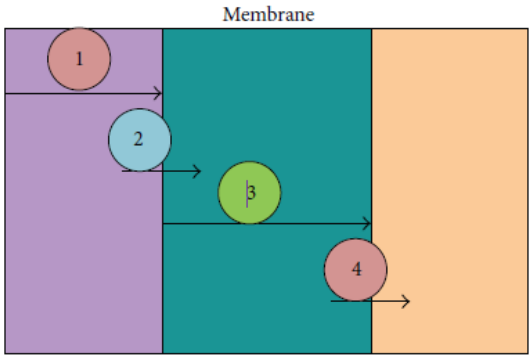

Figure 2.6: Transport steps in solution-diffusion mechanism of component through a pervaporation membrane [17].

2.2.2.2 Factors affecting the pervaporation

When considering about the effectiveness of the pervaporation membrane, it is affected by two parameters mainly. Those are,

- Permeant flux (J).
- Separation factor (β).

These two parameters can be calculated by following equations (Equation 2.1 and Equation 2.2) [18] :

$$J_i = \frac{Q_i}{A\Delta t} \tag{2.1}$$

$$\beta_i = \frac{C_i^a/(1-C_i^a)}{C_i^l/(1-C_i^l)} \tag{2.2}$$

Where J_i is the partial flux of component i ($kg\ m^{-2}h^{-1}$), Q_i is the permeate component i mass (kg), Δt is the operating time (h), A is the membrane area (m^2), C_i^a and C_i^l are the concentrations of the component i in the permeate and the feed respectively.

In order to explain the permeation properties of a membrane, the membrane permeance (P_i^G/l, gpu) ($1gpu = 1 \times 10^{-6}\ cm^3(STP)cm^{-2}s^{-1}cmHg^{-1}$) and selectivity ($\alpha_{ij}$) can be calculated by Equation 2.3 and Equation 2.4,

$$\frac{P_i^G}{l} = \frac{j_i}{P_{i_o} - P_{i_l}} \tag{2.3}$$

$$\alpha_{ij} = \frac{P_i^G}{P_j^G} = \frac{P_i^G/l}{P_j^G/l} \tag{2.4}$$

where j_i is the molar flux of component i ($cm^3(STP)cm^{-2}s^{-1}$), l is the membrane thickness (μm), P_{i_l} and P_{i_o} are the partial pressures of component i on the permeate side and the feed side of the membrane.

Above mentioned factors are affected by [17],

- Membrane thickness
- Temperature
- Initial feed concentration

2.3 Raman spectroscopy

A wide variety of samples can be studied using vibrational spectroscopy and Raman spectroscopy is a technique that is included in vibrational spectroscopy. It can be used to carry out simple identification tests as well as in-depth, full-spectrum, qualitative and quantitative analyses. Several different types of samples can be examined, such as bulk samples, microscopic amounts, or surfaces.

The Raman spectroscopy is required to determine the vibrational modes of a molecule. However, some vibrations are active, and some are inactive in Raman. It is most easily used to study symmetric and nonpolar groups.

This vibrational spectroscopy technique involves the study of the radiation interaction with molecular vibrations. In this process of photon energy is transferred to molecules by changing their vibrational states. The Raman spectroscopy is an inelastic scattering of light that occurs in two photons. The incident photon from a high intensity laser light source, has very higher energy compared to the quantum vibrational energy, and it loses part of its energy due to molecular vibration, with the remainder scattered as a photon of a reduced frequency. Most of the scattering is called Rayleigh Scatter because most of the scattered light is at the same wavelength as the laser source. It will, however, scatter a small amount of light with a percentage of 0.0000001%, in different wavelengths depending on the analyte's chemical structure. This is known as Raman scattering. A molecule's Raman polarizability influences the off-resonance interaction between light and matter.

Several characteristics distinguish Raman vibrational bands [19]:

- frequency (energy)

- Intensity (ability to polarize)
- Shape (bond environment)

The Raman spectrum can be viewed as a "fingerprint" of a molecule since vibrational energy levels are unique to each molecule. The frequencies of these molecular vibrations depend on:

- Atom mass
- shape
- Chemical bond strength

The spectra provide information on:

- Identity and chemical structure
- Phase and polymorphism
- Intrinsic stress or strain
- Impurities and contamination level

Normally, in Raman spectroscopy, the electric field is considered, and the magnetic field component neglected. The most important parameters can be given as wavelength (λ), frequency (υ), and wavenumbers ($\bar{\upsilon}$) which is the number of waves per unit length.

Photons, in quantum theory, are discrete units of radiation emitted by a source, whose frequency, υ, and energy, E_p, are interrelated and can be shown in Equation (2.5).

$$E_p = h\upsilon \tag{2.5}$$

Where h is the Planck's constant (6.6256×10^{-27}erg s). The energy is transferred when photons of specific energies are absorbed or emitted by a molecule. A molecule will be raised from the ground state to a specific excited state in absorption spectroscopy, and it can be illustrated in Figure 2.7.

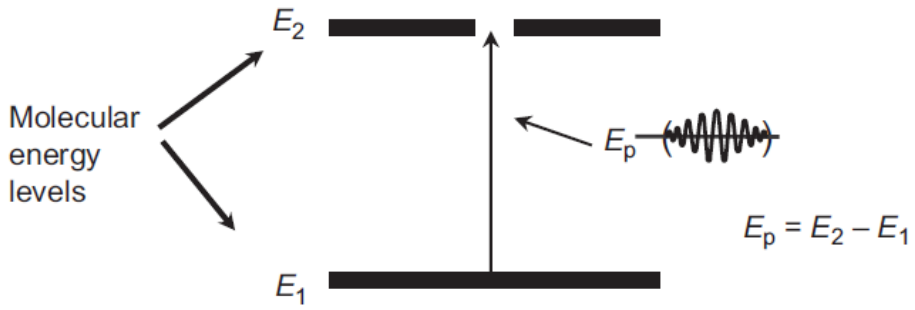

Figure 2.7: Energy increment of a molecule due to energy absorption from photons [19].

A simple model which is derived from classical mechanics can be used to examine the molecular vibrations responsible for Raman bands. Figure 2.8 shows a diatomic molecule with two masses m_1 and m_2 connected by a massless spring. X_1 and X_2 are the displacements of each mass along the spring axis. Harmonic oscillators produce periodic variation due to displacement of the two masses as a sine (or cosine) function of time.

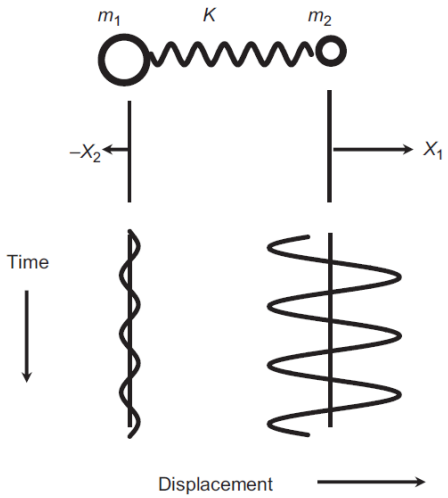

Figure 2.8: Diatomic molecule connected by a massless spring and their displacement with time [19].

Though each mass has different amplitude, both atoms go through their equilibrium positions at the same time with the same frequency in the above diatomic system. The observed amplitudes are inversely proportional to the mass of the atoms which keeps the center of mass stationery, shown in Equation (2.6)

$$-\frac{X_1}{X_2} = \frac{m_2}{m_1} \tag{2.6}$$

A diatomic molecule's wavenumber units, $\bar{\upsilon}$ (waves per centimeter) is given in Equation (2.7):

$$\bar{\upsilon} = 1303\sqrt{K\left(\frac{1}{m_1} + \frac{1}{m_2}\right)} \tag{2.7}$$

Table 2.3 shows the approximated ranges for force constants for single, double, and triple bonds.

Table 2.3: Approximate range of the force constants for single, double, and triple bonds [19].

Type of the bond	K (millidynes/Ångström)
Single	3 - 6
Double	10 - 12
Triple	15 - 18

A diatomic force constant can be calculated based on the mass and frequency of an atom. Larger molecules have complex vibrations, so it is not appropriate to have the harmonic oscillator assumption for a diatomic.

A laser is typically used in Raman experiments to irradiate the sample. Excitation is possible from laser sources of UV, visible, and near-IR spectral range. The Raman scattered light will be visible if visible excitation is used. Figure 2.9 illustrates the Rayleigh and Raman processes. Rayleigh light is not lost through elastic scattering, but Raman scattered photons do lose energy compared to the exciting energy to the vibrational coordinates of the sample. Observation of Raman bands requires polarization to change due to molecular vibrations.

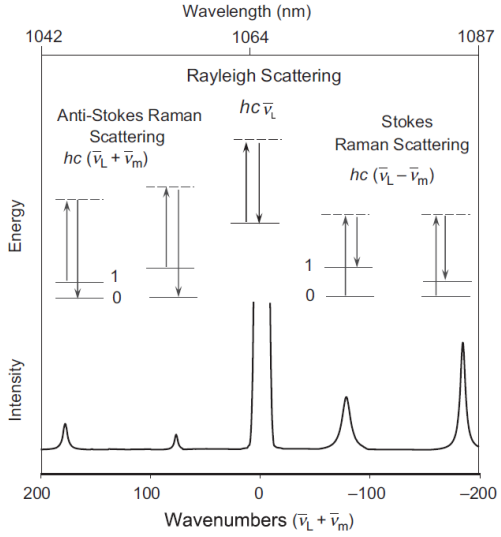

Figure 2.9: Rayleigh and Raman processes [19].

Figure 2.9 illustrates two types of Raman scattering exist Stokes and anti-Stokes. Stokes Raman scattering occurs in molecules initially in the ground vibrational state, $hc(\bar{\upsilon}_L - \bar{\upsilon}_m)$, while anti-Stokes Raman scattering occurs in molecules initially in the vibrational excited state, $hc(\bar{\upsilon}_L + \bar{\upsilon}_m)$.The intensity ratio of Stokes relative to anti-Stokes Raman bands depends on both the absolute temperature of the sample and the energy difference between ground and excited vibrational states. Boltzmann's law is used to describe the intensity ratio of Stokes lines to anti-Stokes lines at a thermal equilibrium. Since most molecules are in the ground state at ambient temperature, Stokes Raman lines are much more intensive compared to anti-Stokes lines.

Several parameters are important for Raman spectroscopy.

- Quantitation is possible since the signal is concentration dependent.
- Raman intensity can be increased by using shorter wavelength excitation or by increasing the density of laser flux.
- Only molecules whose polarizability changes are Raman active.

Raman scattered light will have a wavelength depending on the wavelength of the excitation light, as is evident from the above. Therefore, the Raman scatter wavelength cannot be used

to compare spectra measured with different lasers. By converting scatter position to a Raman shift away from excitation wavelength, the following is obtained:

$$\triangle\bar{\upsilon} = \left(\frac{1}{\lambda_0} + \frac{1}{\lambda_1}\right) \times 10^7 \quad (3.10)$$

Wavenumber Raman shift is given in cm^{-1} while the wavelength of the excitation laser λ_0 and the wavelength of the Raman scatter λ_1 are in nm.

Spectrum profiles provide a unique chemical fingerprint for a chemical component apecially by peak positions and relative peak intensities. Raman spectral libraries have been developed to find matches, thus providing a chemical identification based on the actual spectrum.

Concentration directly affects the intensity of a spectrum. To determine the relationship between peak intensity and concentration, typically a calibration procedure is used, and then the concentration can be determined in routine measurements. When analyzing mixtures, relative peak intensities can give information about relative concentrations, whereas absolute peak intensities can provide information about absolute concentrations.

Before using the data obtained from the instrument for analysis, data should be preprocessed. Normally the effect of fluorescence and other additive properties in the spectrogram are removed by baseline correction. A normalization procedure is done to remove multiplicative effects due to uncertain cases in the reproducible focusing and laser intensity variations [20]. In this project PLS_Toolbox 9.0 (2022) by Eigenvector Research, Inc. in Matlab was used for preprocessing. For baseline correction Whittaker filter was used with Lamda =100 and P = 0.001. It has many advantages such as [21]:

- The ability to program it in Matlab with less than 10 lines.
- Automatic boundary adaptation.
- Ability to handles missing values automatically by a vector of 0-1 weights.
- Ability to smooth even 100 000 observations within few seconds.
- Ability to control the smoothness with one parameter (Lamda).

To normalize data, normalize method was used which can select a portion of the spectra for the normalization. In the instrument used for the analysis of samples in this project, a peak at 750 cm^{-1} can be found and it was solely an instrument peak and therefore Raman shift ranging from 740cm^{-1} to 760cm^{-1} which covers the peaks was used to normalize data. The Figure 2.10, Figure 2.11, and Figure 2.12 shows raw data, the data after applying Whittaker filter and data after applying Whittaker filter as well as normalizing the data, respectively.

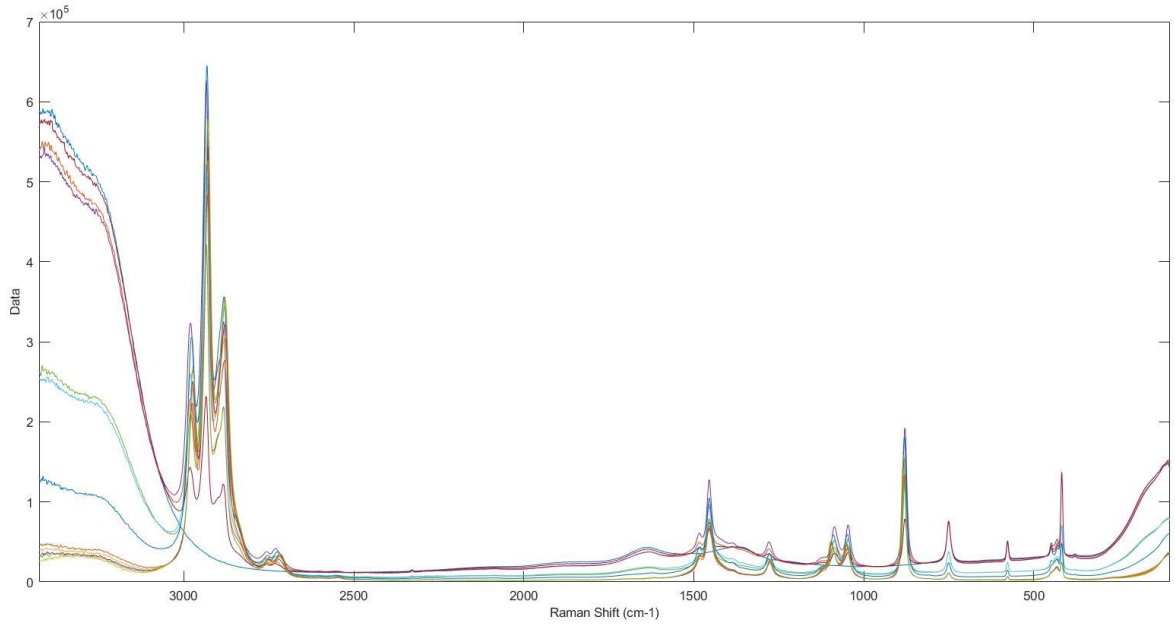

Figure 2.10: Raw data.

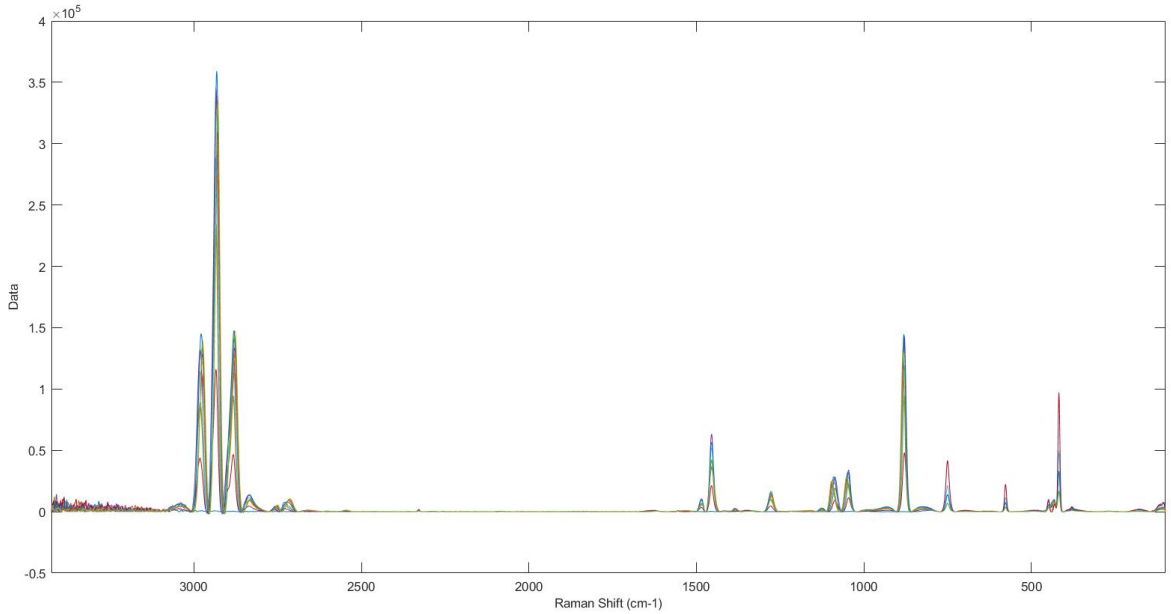

Figure 2.11: Data after applying Whittaker filter.

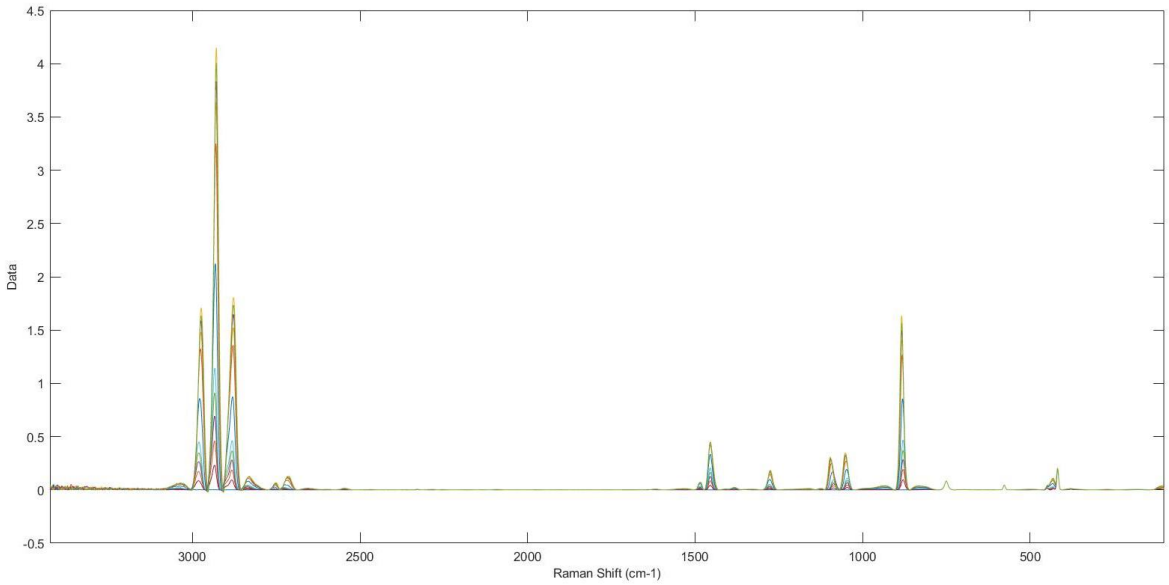

Figure 2.12: Data after applying Whittaker filter and normalization.

2.4 Gas chromatography

Gas chromatography (GC) is able to identify different types of compounds in a mixture and quantify them. It can therefore be used to analyze samples from pervaporation assisted esterification. The following is a brief introduction to GC.

2.4.1 Introduction to gas chromatography

Gas chromatography (GC) is a technique for analyzing gas, liquid, and some solid materials with components vaporized by heat. Using a GC system, it is possible to measure and isolate each constituent of a chemical combination. GC separations are accomplished by a series of sections between a moving stationary liquid phase and gas phase kept in a tube with small diameter after a narrow dose of a mixture is injected [22]. There is a detector which is used to monitor the gas stream composition emerging from the column with different components. The detector's output signals are used as input for data gathering. As well as the GC is used to analyze mixtures that comprise chemicals which have boiling points ranging 0-700 K [22].

2.4.2 GC system and methodology

Equipment used in gas chromatography has undergone several adjustments and advancements since its introduction. Sample injection, column and detector are the three primary GC system components [23]. The functions of main components of a GC system are relatively straightforward as follows.

- Sample injection unit - warms and vaporizes the liquid sample
- Column - separates each chemical
- Detector - detects the compounds and provides their concentrations as electrical signals

The basic components of a typical instrument for performing GC are shown in Figure 2.13.

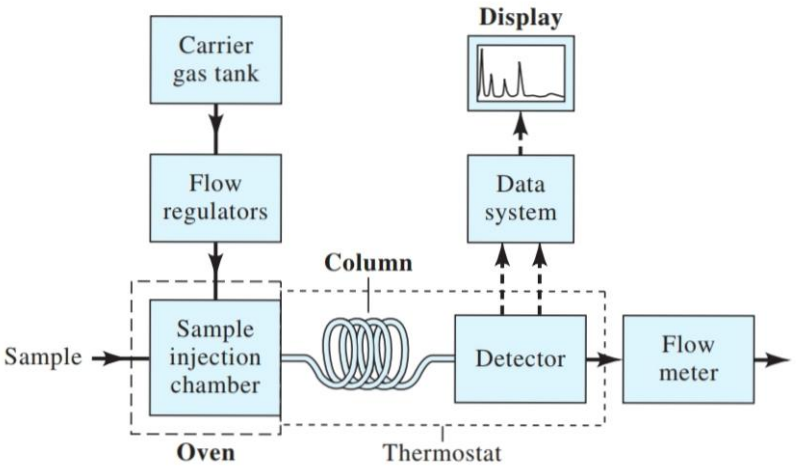

Figure 2.13: Schematic representation of gas chromatography system [23].

In GC, two kinds of columns are used: packed columns and capillary columns. Previously, packed columns were utilized in the great majority of gas chromatographic studies [23]. Capillary columns have mostly superseded packed columns in most modern applications. The mobile phase is injected into the column along with the sample comprising numerous chemicals. The sample and the mobile phase both pass through the column. As a result, the timings at which the various compounds arrive at the column output varies. As a result, each component separates from the others [23].

2.4.3 Graphical analysis

A chromatogram is a row of peaks generated after separation when the electrical impulses emitted from the GC detector are displayed on the y axis and the elapsed time after sample injection is represented on the x axis. Figure 2.14 depicts a typical chromatogram.

The horizontal axis represents the time it would take for the constituent to reach the detector. The signal intensity is shown on the vertical axis. The area when nothing is detected is referred to as the baseline, while the part where a component is discovered is referred to as the peak. The retention time is the period between when the sample is put into the system and when the peaks show. Each component can be isolated and recognized since their elution periods differ [24].

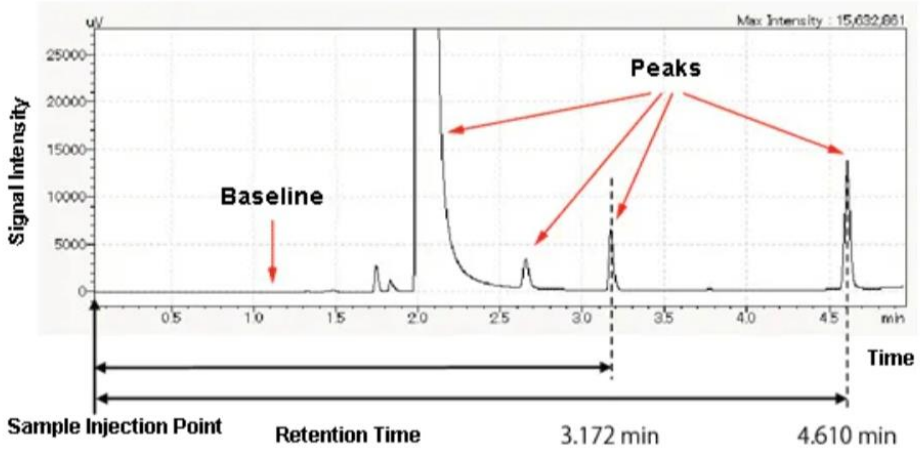

Figure 2.14: A typical chromatogram [24].

The area of the component peak in a GC are equivalent to the amount of the constituent which approach the detector [25]. As an example, a quantitative study of component A concentration in an unknown sample is given. Suppose that 1 µL of the unknown sample is examined and the area of the peak for component A in the acquired chromatogram has a value of 700. Following that, a standard sample is required to identify the unknown quantity of a desired component, and it is created with a component A concentration of 100 ppm. 1 µL of this is evaluated under the identical circumstances, and a peak area of 1000 is recorded. Figure 2.15 the pictorial representation of this case study. The peak size is proportional to the amount of the component, therefore if a concentration of 100 ppm has a count of 1000, a count of 700 it indicates that concentration is 70 ppm.

Therefore, a standard sample is important for both quantitative analysis and qualitative analysis [25].

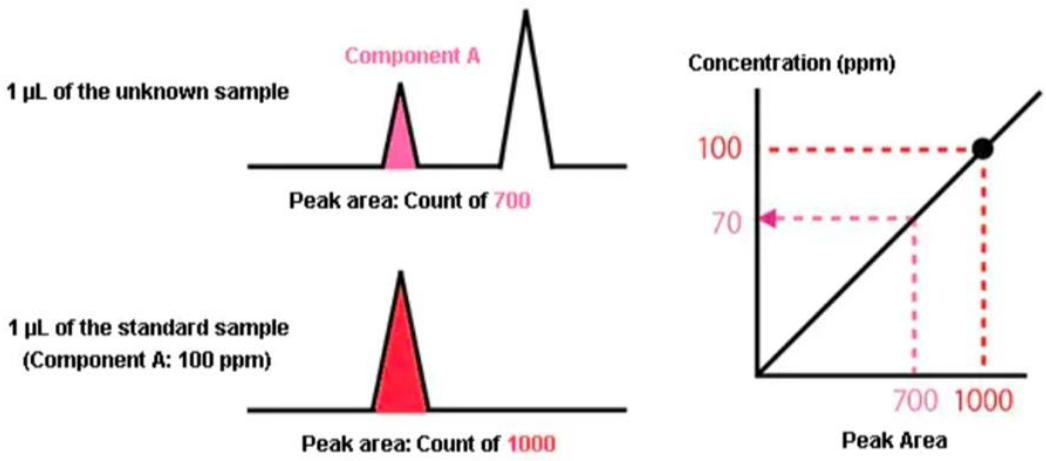

Figure 2.15: Schematic representation of gas chromatography system [25].

3 Literature review

In this chapter a literature review was done for pervaporation membranes used in esterification and the conditions that affect the pervaporation assisted esterification.

3.1 Pervaporation membranes for esterification

It was the hydrophilic membranes that first achieved industrial use for pervaporation and were used to dehydrate organic solvents. It is still the dehydration of organic liquids that accounts for the majority of industrial applications of pervaporation, as before. Changing the chemical composition and structure of the active layer of these membranes allows them to extract water with a wide range of flux and selectivity [26, 27]. Polymeric membrane materials used in commercially available hydrophilic membranes include polyvinyl alcohol (PVA), Nafion, polyimides, polyacrylonitrile (PAN) and polymaleimides.

In recent years, a number of researchers have been engaged in research and development of hydrophilic membranes, which can be categorized into organic, inorganic, and organic-inorganic hybrid membranes. Zeolites and silica are the commonly used inorganic membranes [28, 29]. These membranes are generally prepared by the sol-gel method [30] and are suitable for applications with high temperatures (or harsh environments). Despite their high dehydration efficiency, these inorganic membranes are unlikely to be industrialized quickly because of their high manufacturing costs and complex large-scale preparation. A number of commercial organic membranes have also been introduced to the pervaporation assisted esterification, including, PERVAP 1005 (GFT) [31] and PERVAP 2201 [32, 33]. Several studies have also been conducted on cross-linked PVA membranes, including PVA using the catalyst Amberlyst and $Zr(SO_4)_2.4H_2O$[34, 35], on polyethersulfone [36, 37], and on poly(acrylonitrile) [38]. Nevertheless, these organic membranes are inherently unstable, severely limiting their use.

A hybrid of organic and inorganic compounds has been proposed as having both the organic functionality and inorganic stability. To increase the yield of ethyl lactate, Budd et al.[39] used multilayer pervaporation membranes composed of zeolite and polyelectrolyte (chitosan/poly(4- styrene sulfonate)). Adoor et al. [40] prepared sodium alginate pervaporation membranes with aluminum-rich zeolite beta incorporated into them. An organic-inorganic hybrid membrane produced better flux and retention with pervaporative dehydration.

The pervaporation of water through hydrophobic membranes separates volatile organic compounds from the water. Polymeric hollow fiber membranes are used in hydrophobic membrane systems. Water molecules are rejected by the membrane since they are hydrophobic and only permit volatile organic compounds. Polymeric membranes are typically used in high-value products, such as aroma compounds and organic compounds separation, such as pollutants. Ceramic membranes [41, 42] are occasionally also used. Polymeric membranes, as well as ceramic membranes, have low selectivity for recovering polar volatile organic compounds from very dilute solutions [43, 44]. Polydimethylsiloxane (PDMS) is one of the most commonly used polymers for organic compound separation. In light of the flexible structure, Polydimethylsiloxane demonstrates high permeability and selectivity towards organic compounds, and therfore suitable for removing organic compounds from water [45].

A typical example of pervaporation being used to remove a byproduct or a product of a reaction in a hybrid reactor configuration is esterification. Several types of commercial membranes can be used in pervaporation-esterification coupling systems, including PERVAP 2201 [32, 46], PERVAP 1005 [47, 48], GFT-1005[49] and polydimethylsiloxane [50]. A comparison of the various membranes used for pervaporation-assisted esterification is presented in Table 3.1.

Zhang et al. [10] used three types of synthetic membrane in his study, carbomer (CP)/glutaral cross-linked chitosan (GCCS)/PAN, glutaral cross-linked hyaluronic acid (GCHA)/hydrolysis modification- (HM-) PAN and glutaral crosslinked gelatin (GCGE)/PAN. Korkmaz et al. [51] studied the esterification of acetic acid with isobutanol using water permeable PVA membranes and ester permeable PDMS. To increase the conversion of the esterification reaction, Zhang et al. [52] incorporated a catalytically active pervaporation membrane. It had three layers: a porous catalytic layer on the surface, a separation layer (PVA membrane) and a support layer (PES porous membrane).

Table 3.1: Summery of various membranes used for pervaporation-assisted esterification.

Esterification reactions	Membranes	Nature of membrane	Reference
Lactic acid + ethanol	Chitosan-tetraethoxysilane hybrid membrane	Hydrophilic organic-inorganic hybrid membrane	[53]
Acetic acid + methanol	Nafion membrane	Hydrophilic catalytically active membrane	[54]
Acetic acid + butanol			[54]
Lactic acid + ethanol	GFT-1005 and T1-b membrane	Hydrophilic organic membrane	[49]
Succinic acid + ethanol			[49]
Acetic acid + isobutanol	Polydimethylsiloxane membrane [PDMS]	Hydrophobic cross-linked membrane	[55]
Acetic acid+ ethanol			[50]
Lactic acid + ethanol	PERVAP 2201	Hydrophilic polymeric membrane	[32]
Lactic acid + ethanol	PERVAP 2201		[56]
Acetic acid + isopropanol	PERVAP 2201		[44]
Lactic acid + ethanol	PERVAP 2201		[57]
Acrylic acid + n-butanol	PERVAP 2201		[58]
Lactic acid + ethanol	PERVAP 2216		[57]
Acetic acid+ isopropanol	PERVAP 2201		[46]

Propionic acid + isopropanol	PERVAP 2201		[59]
Oleic acid + i-amyl alcohol	PERVAP 1005		[48]
Acetic acid+ ethanol	PERVAP 1005		[31]
Acetic acid + benzyl alcohol	PERVAP 1005		[47]
Acetic acid + ethanol	PERVAP 1000		[9]
Oleic acid + ethanol	PERVAP 1000		[60]
Acetic acid + ethanol	Polyetherimide-γ alumina composite membrane	Hydrophilic composite polymeric-inorganic membrane	[61]
Lactic acid + ethanol	Silica membrane [Pervatech BV]	Hydrophilic inorganic membrane	[28]
Acetic acid+ ethanol	Polyetherimide composite membrane	Polymeric/ceramic membrane	[62]
Acetic acid + n-butanol	PVA membrane	Hydrophilic polymeric/ceramic composite membrane	[63]
Acetic acid + butanol	PVA membrane cross-linked with catalyst $Zr[SO_4]_2 \cdot 4H_2O$	Polymeric composite catalytic membrane	[34]
Acetic acid + butanol	PVA membrane [Amberlyst coated]	Polymeric/ceramic composite membrane	[35]
Oleic acid + methanol	PVA membrane [cast on polyether sulfone]	Hydrophilic polymer composite membrane	[36]
Methacrylic acid + 2,2,2, Trifluoroethanol			[37]
Acetic acid + ethanol	Zeolite membrane [aluminum rich zeolite	Hydrophilic mixed matrix membrane	[40]

	beta incorporated sodium alginate]		
Acetic acid + n-butanol	Zeolite T membrane	Hydrophilic membrane	[64]
Acetic acid + ethanol			[65]
Lactic acid + ethanol	Zeolite NaA membrane	Hydrophilic membrane	[29]
Propionic acid + isopropanol			[6, 66]
Acetic acid + n-butanol	Poly[ether block amide]membrane	Organophilic membrane	[6]
Acetic acid + methanol	Poly[2,6-dimethyl-1,4-phenyleneoxide] [PPO]and thin layer fluoroplastic	Hydrophobic composite membrane	[67]
Acetic acid + ethanol	Tubular hydroxy sodalite [SOD] membrane	Hydrophilic membrane	[68]
Acetic acid + butanol			[68]
Acetic acid + ethanol	HZSM-5 membrane	Hydrophilic catalytic active membrane	[69]
Acetic acid + ethanol	Poly[2,6-dimethyl-1,4-phenyleneoxide] [PPO]and fullerene C_{60}	Hydrophobic composite membrane	[70]
Acetic acid + ethanol	Hydrophilic membrane	Hydrophilic membrane	[71]
Lactic acid + ethanol	Water selective	Hydrophilic membrane	[72]

	membrane		
Lactic acid + isopropanol	PVA-PES composite membrane	Hydrophilic cross-linked membrane	[73]
Lactic acid + n-butanol	PVA-PES composite membrane	Hydrophilic membrane	[74]
Acetic acid + ethanol	PVA-PVP incorporating PMA mixed matrix membrane	Hydrophilic membrane	[75]

3.2 Operating conditions effect on esterification with pervaporation

Operating parameters can be divided into three groups [76]:

1. The initial reactant molar ratio (alcohol: acid) and the catalyst concentration are factors that directly affect the esterification kinetics.
2. Membrane area to initial reaction volume ratio (A/V_o) has a direct impact on pervaporation kinetics.
3. Temperature influences both esterification and pervaporation kinetics simultaneously.

3.2.1 Initial reactant ratio

A study by Delgado et al. [32] examined ethanol: lactic acid initial feed molar ratio (R) effect with catalyst loading (Amberlyst 15) 2%, surface area to initial volume of reaction ratio was 23 m^{-1} (PERVAP 2201), and pervaporation and reaction temperatures of 348.15 K. A higher initial reactant molar ratio indicated a faster reaction rate at the beginning of the process. In the course of the reaction, higher ester formation was observed when the reaction was carried out in a stoichiometric proportion. Perhaps ethanol's dilution effect is responsible for this. As reaction molar ratios increased in the esterification reactions, equilibrium conversions were high. It is possible to obtain complete conversion of one reactant when the other reactant is excess in esterification-pervaporation reactors, regardless of the size of the excess. An integrated process like this can convert beyond equilibrium, whereas in a conventional reactor it can max out at equilibrium. Pervaporation-assisted esterification of n-butyl alcohol and acetic acid with catalyst, Xuehui et al. [77] have demonstrated ester formation is high at high R (R = initial molar ratio of alcohol to acid). The maximum weight percentage of water is also achieved at low time periods when the R is high. In their study, Liu et al. [78] calculated F, the ratio of water removal to water production during the pervaporation assisted esterification process, which used PVA/ceramic composite membrane. The conversion rate increased, and the water production rate decreased as R grew. In the mixture, the maximum water content had a larger amplitude at a lower R.

Ma et al. [53] found that ethyl lactate yield didn't significantly increase with an increase in alcohol to acid molar ratio from 2 to 4. PV kinetics were unaffected by R, but it influenced reaction rate. As R increases, water production rate decreases, resulting in a lower maximum amplitude of water content.

3.2.2 Catalyst concentration

Domingues et al. [47] was able to find with acetic acid and benzyl alcohol in esterification, with a GFT membrane, an increase in the amount of catalyst is associated with a higher reaction rate; however, beyond 4.1 mol/m^3, the increment of the rate is insignificant. The water production rate was proportional to catalytic concentration, and it increased with an increase in catalytic concentration in the experiment by Liu et al. Catalyst concentration rise increased the maximum water content and shifted the mixture to shorter time periods, which resulted in decreased final water content. Using an organic/inorganic hybrid membrane, Ma et al. [53] varied the catalyst concentration 0.5 wt% - 3.0 wt% in ethanol and lactic acid esterification reaction. Increased catalyst loading improved ethyl lactate yield. It is due to an

increase in catalyst active sites in the solution mixture and due to this reduced activation energy in the reactions, resulting accelerated reactions. For a higher catalyst concentration in the reactor, the water content had a higher maximum amplitude. Using PERVAP 2201, Delgado et al. [32] investigated the effect of catalyst concentrations (5.5%, 3.5%, and 2% on weight basis) in esterification of ethanol + lactic. The reaction rate increases with the amount of catalyst used. Due to the large amount of water at the beginning of the reactor, the effect of dilute acid is not higher.

3.2.3 Membrane area to initial reaction volume ratio

Using Amberlyst 15 and PERVAP 2201 when esterifying ethanol and lactic acid, Delgado et al. [32] varied the ratio, area: initial reaction volume. According to this study, the higher this ratio is, the more ethyl lactate is formed in the reactor, triggering the highest conversions. Due to the larger area of membrane per unit of reaction volume, the water concentration will decrease faster in the reactor. In studies on acetic acid and benzyl alcohol with catalyst, it was able to achieve 60% conversion of acetic acid, Domingos et al. [47] found that an increase in surface area of membrane (S) can result in a reduction in operating time. Additionally, alcohol was converted to 100 percent. The membrane parameter (characterizing membrane permeability (ω)) and the operating parameters S and V_o (surface area/volume of reaction mix) are combined to measure the membrane unit's capacity [79]. The membrane reactor showed the ability to convert beyond its equilibrium conversion. As reaction time increases, the gap between the two limits, i.e., ωS/V varies from 0 to infinity, becomes larger, indicating that membrane pervaporation facilitates the reaction more and more. For higher $\omega S/V$ value, the higher the conversion can be achieved. As the reaction proceeds in time, the water concentration (C_w/C_o [C_w is the concentration of water and C_o is the concentration of water obtained at complete conversion]) reaches its peak. With a larger ωS/V ratio, water will reach maximum concentration in a shorter time and with a smaller magnitude. Reaction rate decreases with the progress of the reaction. The use of a membrane can, however, prevent a reduction in reaction rate since the removal of water improves the concentration of the reactants. Even though for a large value of ωS/V, pervaporation cannot force the reaction to completion, that is, X = 1, even if the equilibrium shifts to the ester. In excess of one of the reactant species, the other can be completely converted.

It was explained that when a membrane is more permeable or when it has larger area per unit reaction volume, the concentration of water will be decreased quickly in a reactor, thus increasing the conversion. Chemical reaction rates are high early in a reaction, while the amount of water in the reactor and rate of water removal are low. The result is that the concentration of water gradually rises until a maximum is reached and at that point the formation and the removal rates are similar. Afterward, the water is removed at a higher rate than it is formed, resulting water depletion in the reactor.

A study by Liu et al. [78] showed that as S/V decreased the water removal rate also reduced. Further, the amplitude of the liquid was higher at a lower S/V. According to Ma et al. [53], S/V did not affect the reaction kinetics but affected the water extraction rate. As S/V increases, water production rate decreases.

3.2.4 Temperature of pervaporation and reaction

Delgado et al. [32] investigated ethanol and lactate esterification utilizing PERVAP 2201 membrane was able to find that the water amount decreased rapidly after increasing permeation flux due to increased temperature. Esterification rates increase as a result. Based on Xuehui and Lefu's report, higher ester amount is formed at higher temperatures. The maximum water concentration is also received for low temperatures.

It was discovered by Liu et al. [78] for acetic acid, n-butyl alcohol with $Zr(SO_4)_2.4H_2O$ and PVA/ceramic composite membrane, that water removal to water formation ratio increases with increasing temperature, illustrating higher rates of water removal through membrane than water production from the reaction. At a higher temperature, the permeability coefficient and production of water are both higher. Temperature increased maximum concentration of water, but the maximum time was shortened due to higher production rates. Until the water content reached its highest value, the water formation rate exceeded water removal rate. Once the water amount reached the maximum, water production rate decreased.

Utilizing an organic-inorganic hybrid membrane, Ma et al. [53] performed experiments for temperatures between 50°C and 80°C. Based on Arrhenius plots, the esterification reactions were endothermic for ethanol and lactic acid; therefore, the ethyl lactate yield increased with increasing reaction temperature. Liu and Chen found that function of process temperature can present reaction rate constants for the esterification and increment can be seen with the increase of temperatures (70–90°C). In the forward reaction, the reaction rate constant increased more rapidly with temperature increase than in the backward reaction. In other words, the rate of water production is high in a high temperature. Furthermore, the permeation parameter of water is also affected by temperature and increases with a rise in temperature. Due to the increase in process temperature, water permeation flux increased. The maximum concentration of water increased with an increase in process temperature. The reason for this might be that at higher temperatures the acceleration for water formation rate was higher as well, so at early stage of the reaction, water content rapidly increased because of the sluggish backward reaction rate

Grob and Heintz [80] investigated the behavior of aromatic compounds with organophilic polymer membranes (polyetherpolyamide block-copolymer (PEBA)), used in pervaporation. They were able to find that the sorption of phenol, 4,4-isopropylidenediphenol (bisphenol A), 2-chlorophenol, pyridine, 4-nitrophenol, aniline, and 2,4-dinitrophenol to decrease with temperature. The slopes of straight lines give the sorption coefficients. An aromatic compound's affinity for PEBA is influenced by the number of free hydroxyl groups in it. Exothermic sorption occurs when aromatic compounds are transferred from aqueous solution to the membrane. Calculated sorption enthalpies $\Delta h_{\text{infinity}}$ range between -25 and -12 kJ/mol. The presence of the second aromatic compound did not affect the sorption of aniline and phenol in the membrane material. Synergistic solubility effects are seen in the phenol/bisphenol A system. Bisphenol A enhances the solubility of phenol, but phenol does not affect bisphenol A's solubility, Burshed et al. [81] investigated the pervaporation of glycerine-water mixtures using membranes such as carboxylated polyvinyl chloride, Nafion, polyimide cellulose triacetate and polyethersulfone. During the experiment, the temperature varied between 30 and 70°C. According to the research, higher feed temperatures decreased water sorption, so sorption heat (ΔH_s) is negative.

3.2.5 Other factors

3.2.5.1 Downstream pressure (permeate side vacuumed pressure) effects on various Terms

Desorption is slowed down at membrane permeant interface if downstream pressure increases; therefore, downstream pressure becomes a rate determining factor. Selectivity decreases as pressure increases beyond the saturated vapor pressure of permeance. Low vacuum pressures result in fast desorption, so diffusion becomes the rate determining factor. The rate of desorption slows down beyond the transition pressure and gradually determines the selectivity of pervaporation. Selectivity is governed by the relative volatility of feed components in this regime. Selectivity increases as the downstream pressure increases if the permeating component is also high volatile. Selectivity decreases in the opposite case. Permeant composition depends on downstream pressure for ideal gas mixtures with no significant amounts of non-condensable gases.

Burne et al. [81] investigated the effect of downstream pressure on the dehydration of glycerine water mixtures using various membranes. The pressure ranged from 1 to 20mmHg. A higher downstream pressure resulted in a lower water flux. Downstream pressure has no effect on selectivity. By using 20mmHg downstream pressures, the refrigeration unit supplying the cooling medium for condensing the water issuing from the equipment is reduced to a lesser degree.

3.2.5.2 Molecule size on the permeability

Using a surface-modified alumina membrane (Al_2O_3), Song et al. [82] examined the pervaporation of ethyl propionate, ethyl acetate and ethyl butyrate. As the concentrations of esters in the feed stream increased, the concentrations of esters in the permeance approximately linearly rose. While molar volume and molecular weight of ethyl butyrate are greater than ethyl propionate and ethyl acetate, the permeance ester concentration and ester flux improved in the order of ethyl butyrate > ethyl propionate > ethyl acetate. Because of EB's low solubility in water, this may be attributed to its high hydrophobicity. Since ethyl butyrate has the smallest solubility, it has the largest affinity for the surface of the membrane since it is hydrophobic. Since organic components have a strong affinity for the organophilic membrane than dilute solutes, this is to be expected. Despite Esters' presence in feeds only amounting to 0.15 – 0.60wt%, in permeance Esters reached concentrations of 9.13 – 32.26, 13.79 – 37.0, and 15.33 – 42.57wt%. The ester concentration in the permeant stream was much higher than the saturation limit, resulting in phase separation.

Different components have different affinities for the membrane, which is why their flux and permeance in a given membrane differ. The solubility parameter can be used to describe the affinity between materials. In a study of the dehydration of butanol mixtures, Guo et al. [83] determined that the solubility parameters δ_{sp} of water and the selective layer of the membrane are 47.9 and 39.1. Based on the solubility parameter theory, a strong interaction should occur when the solubility parameters are similar. This theory predicts that the affinity between 1-butanol and the membrane is greater than that between isobutanol, 2-butanol, and tertbutanol.

Hasanoglu et al. [84] studied polydimethylsiloxane (PDMS) effects on the hydrolysis reaction of water, ethanol, acetic acid and ethyl acetate. Ethyl acetate is far more permeable through the PDMS membrane than the other components. Due to PDMS's solubility parameter being close to ethyl acetate (δ_{PDMS} = 8.1 $(cal/cm^3)^{0.5}$) [85], this is not surprising. The PDMS

component is therefore more selective than other components to ethyl acetate. In addition, the solubility parameter can provide information regarding the interactions between the permeate and the polymer. By increasing the affinity between the penetrant and polymer, the quantity of liquid in the polymer will increase, leading to a greater flux through the membrane [86].

4 Experimental studies

Experiments were performed in an experimental setup specifically constructed for the project. The main purpose of the experimental studies was to observe water separation from a mixture of organic compounds via a membrane separator.

This chapter will initially look at the experimental set-up that was used and the construction of the experiment setup. After that, the experimental procedure and the analytical technique will be presented.

4.1 Experimental setup

All experiments were conducted in a pervaporation reactor (PVR). The reactor consisted of a membrane separator module (SEPA® CF membrane cell) and a three-neck glass reactor. For trapping and condensing the volatiles in the feed, the glass reactor had a reflux condenser. Using a silicone oil heating bath heated by a heater (Heidolph MR Hei-End hotplate with magnetic stirrer) integrated with temperature measuring probes, a temperature within the accuracy of $\pm 10^{o}C$ (minimum ΔT available in the heater) was maintained inside the glass reactor. A magnetic stir bar was used to mix the feed solution properly. Centrifugal pumps transferred feed solution from the glass reactor to the PVR module. The PERVAP™ 4100 membrane was fixed to the middle of the PVR module. To control the temperature of the PVR module, it was placed inside an oven (Termaks oven). On the permeate side, the vacuum pressure was applied by a vacuum pump (Vacuubrand® Chemistry-HYBRID pump RC 6), and the liquid that permeated through the membrane and evaporated due to the vacuum pressure was condensed and collected in a cold trap. Figure 4.1 shows the rig in its entirety, and Figure 4.2 shows the schematic of the PVR setup.

Figure 4.1: Experimental setup.

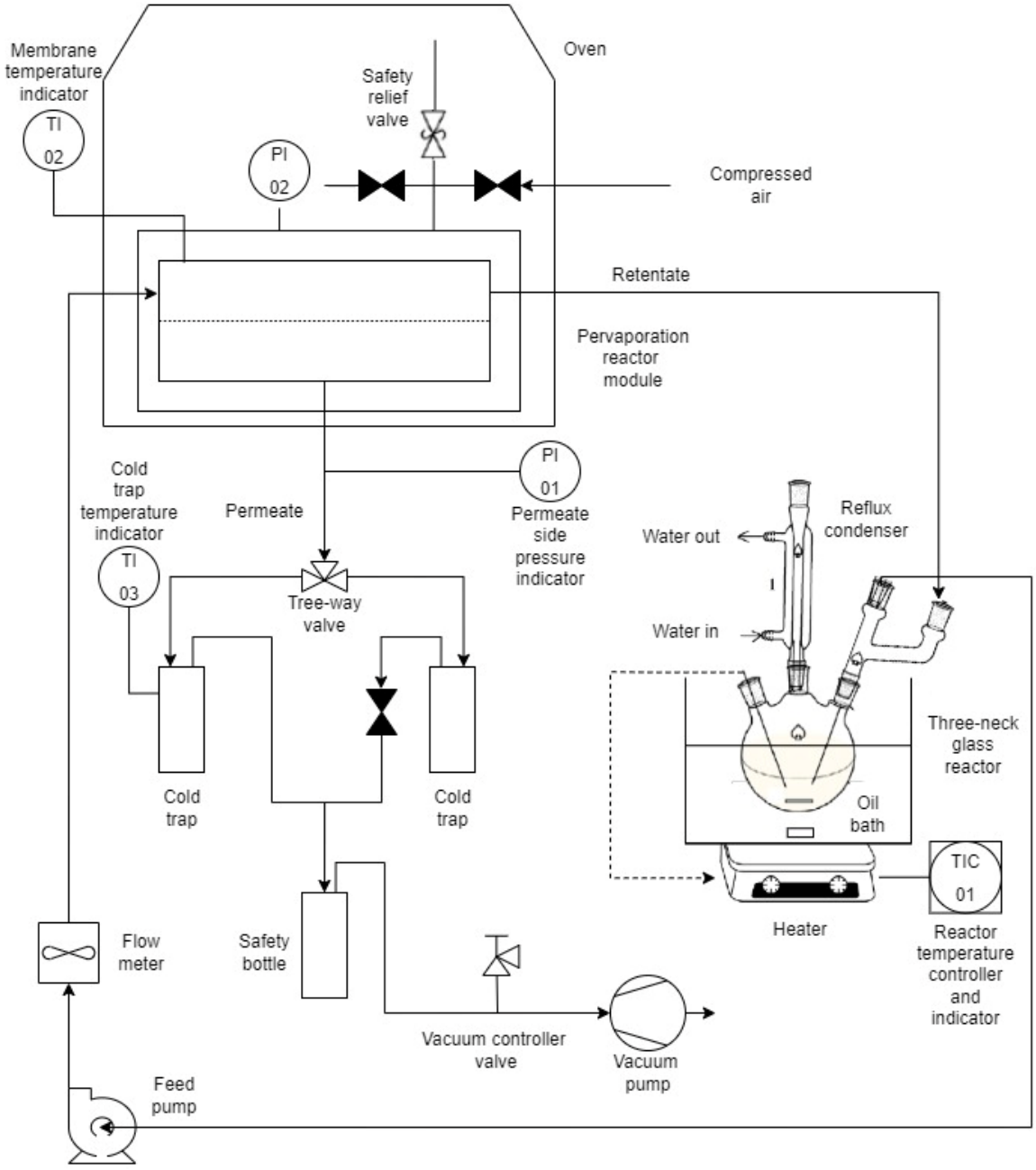

Figure 4.2: Schematic of the PVR setup.

4.1.1 Experiment setup construction

A major part of the available time for the project was consumed by setup construction. This is because it needed to be built from scratch with available resources and even though the experiments in the literature have schematic diagrams, the construction of such an apparatus was not described in detail in the literature. Therefore, it is an entirely new area to explore in this project. The supervisors' knowledge of systems closer to this and their expertise in building an experimental setup were immensely helpful. Below is a description of how the experimental setup was constructed in several parts.

4.1.1.1 Components collection

Collecting the components was a major step in setting up the experimental setup. A membrane separation module was provided, as well as instruction manuals for the module. Also provided were testing membranes which were used to test the apparatus. At an early stage of the project, new membranes for the project were delivered. Several of the tubing needed could be found in the CO_2 laboratory and the Chemistry laboratory, and some was provided by the supervisors. Tubing diameters were largely determined by the available components in the apparatus and the pressures of the streams. In many places, Swagelok fittings were used for airtight connections. The glass wear required was found in laboratories and storages.

4.1.1.2 Three neck glass reactor construction

A three-necked glass bulb was used for the reactor. There were glass tubes with the right diameter that could fit the tubing for the feed and return streams. A reflux condenser that fits the three-neck glass reactor was found and used with flexible vinyl tubing that transported the water stream in and out of the condenser. The condenser and the reactor were connected using plastic clips. A temperature measuring probe was used to measure the temperature in the feed and control the temperature in the silicone oil bath by regulating the heating element in the heater. Magnetic stirring bars were employed to mix the liquid mixture in the reactor as well as the oil in the oil bath in order to transfer the heat received from the hot plate more efficiently. The fittings and the openings were sealed with tight gaskets and vacuum grease to prevent vapor leaks. Figure 4.3 shows the three-neck glass reactor.

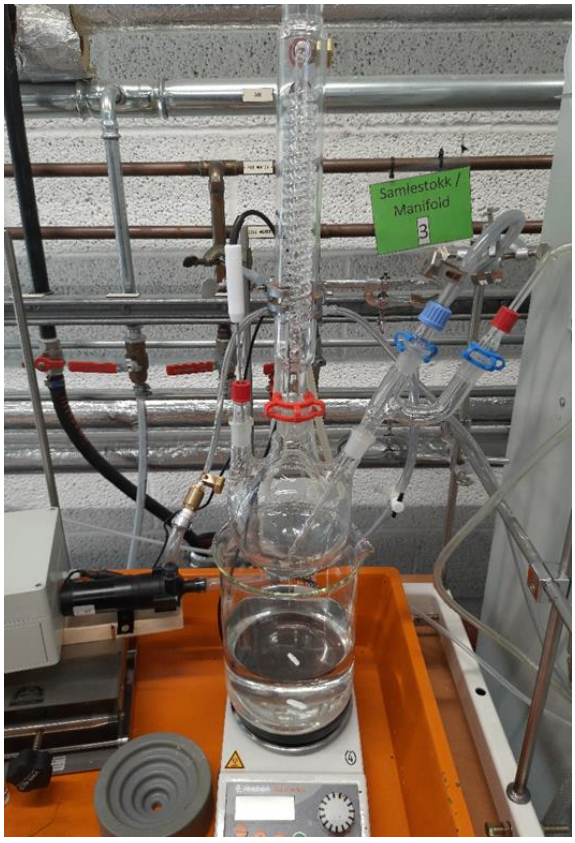

Figure 4.3: Three neck glass reactor.

4.1.1.3 Pervaporation reactor construction

The membrane separator module with a cell holder was used for pervaporation. The cell holder should be supplied with compressed air so it can clamp the membrane separator with an inbuilt piston. For this purpose, reinforced PVC hose was used to supply the air from the compressed air system, and it could withstand 18 bars maximum pressure at 20^{o}C [87]. The compressed air system at the university maintains a constant pressure of 8 bars. Therefore, the reinforced PVC hose selected was more than adequate for the application. Swagelok fittings were used again here for connecting the hose to the membrane holder. After the reinforced hose, an on-off valve was used to disconnect the compressed air system from the membrane holder whenever needed. To release compressed air from the membrane cell holder, another on-off valve was connected to a four-way connector fitting which was connected to the compressed air supply. A safety relief valve was also connected to the four-way connector fitting. It was calibrated to release pressure at 8.5 bars. The membranes and permeate carriers were cut to the proper size to fit into the membrane cell. There was a feed spacer available for the membrane cell that was used during the experiment. Previously used O-rings in the membrane cell were used here because there were no leaks, and the vacuum could be held. It was necessary to create a vacuum in the permeate side in order to create the driving force required and to remove the permeate from the PVR. Figure 4.4Figure 4.3 shows the PVR below.

Figure 4.4: Pervaporation reactor.

4.1.1.4 Sampling system construction

As part of the experiment, samples were collected mainly from the three-neck reactor and the permeate was also collected. It was also possible to collect spot samples from the permeate. To direct the vapor from the membrane cell to either the continuous sampling bottle or the spot sampling bottle, a three-way valve was used. The continuous sampling bottle was always under vacuum, whereas the spot sampling bottle could be isolated from it. This is because the spot sampling bottle needs to be changed each time a sample is taken. After taking a spot sample, the spot sampling bottle could be replaced by a new one since it can be isolated.

As the permeate side is under vacuum, the liquid that passes through the membrane vaporizes immediately. This vapor condenses at low temperatures. To avoid losing permeate through the vacuum pump and collect it, the permeate should be cooled to subzero Celsius temperatures where it could condense under vacuum. The condensing temperature depends on the vacuum pressure and the composition of the permeate. To collect the permeate, a cold trap was set up. The ice with salt was used for the cold traps. Swagelok PFA flexible tubing was used from the permeate side of the membrane cell to the vacuum pump since the tubing should be able to withstand external pressure without collapsing. To maintain the vacuum inside the system, tight gaskets and high vacuum grease were used. In order to control the vacuum pressure, a needle valve was attached with one end open to the atmosphere. By using a needle valve, the opening to the environment could be adjusted slightly and vacuum pressure needed inside the system could be created. Figure 4.5Figure 4.3 shows the sampling system.

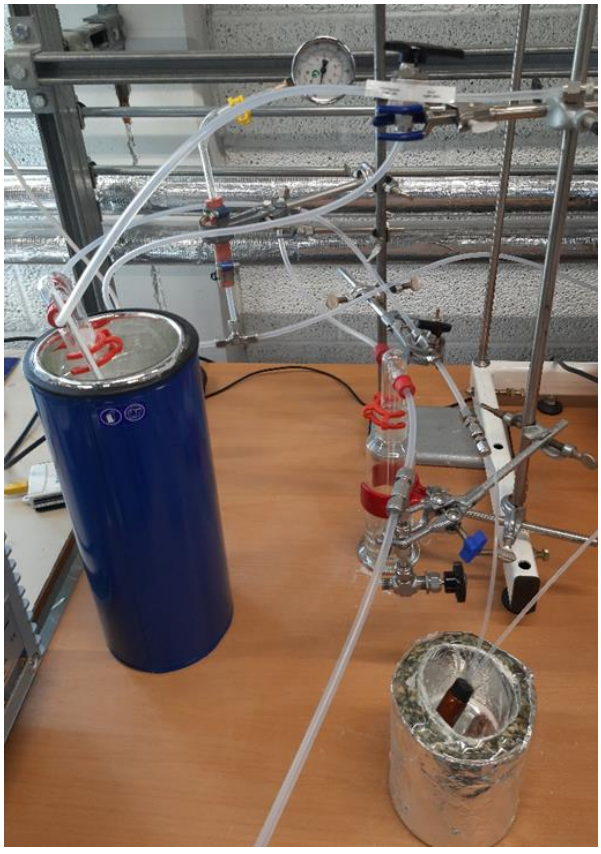

Figure 4.5: Sampling system.

4.1.1.5 Feed pumping and retentate recirculating system

The transfer of fluid between the glass reactor and PVR was accomplished using flexible polymer tubes. These tubes could withstand the temperatures encountered during this project. The tubes were connected to the membrane cell with Swagelok fittings. The polymer tubes were connected to the glass reactor with glass tubes. A centrifugal pump was used to pump the feed, and the flow rate could be controlled by the pump. The flow rate of the feeding liquid was measured by a flow meter installed after the pump discharge. To calculate and display the flow rate, a LabVIEW program was developed. The flow meter needed to be calibrated before being used in experiments.

4.2 Experimental procedure

One of the main objectives described in the introduction was to use the ethyl acetate synthesis esterification reaction as a model equilibrium reaction in the PVR. Unfortunately, due to complications during the project, experiment plans had to be revised accordingly to observe membrane separation of water from water-ethanol mixtures where water separation could be observed.

Here is an explanation of the materials used, the experiments followed, the analysis techniques used, experiments plan and the reasons for the change in plans.

4.2.1 Materials

Ethanol (99.9%) obtained from Antibac® and distilled water was used for the experiments and for the solutions required for analysis of the product.

As it is discussed in theory section and literature study section, polyvinyl alcohol (PVA) hydrophilic membranes are suitable for the model reaction chosen in the project. Therefore, a polymeric hydrophilic membrane (PERVAP™ 4100) which contains a cross linked, active PVA separation layer, was used in the experiments. It was obtained from the DeltaMem AG (Allschwill, Switzerland). Table 4.1 indicates the operating conditions of the membrane.

Table 4.1: operating conditions of the membrane.

Parameter	Operating condition
Maximum temperature of feed	Short term – 107^{o}C Long term – 105^{o}C
Viscosity of feed	Up to 5cP
Suspended solids in feed	Pre-filtration with a 3-4 µm filter (otherwise can have a detrimental effect on membrane performance)
Dissolved solids in feed	<10ppmw total solids from dry residue analysis at 110-130^{o}C (otherwise can have a detrimental effect on

	membrane performance)
Melting point of permeate	Below 0^{o}C (Compounds which solidify on the permeate side can result in reduced membrane flux over time)
pH in feed	5 - 8
Maximum water concentration in feed	Up to 50% w/w

4.2.2 Experimental procedure

The membrane separator was preheated in the oven to reach operating temperature before the experiments began. In addition, the three naked glass reactor was also preheated in the oil bath to reach the operating temperature. A mixture of crushed ice and salt was prepared for the experiment. Before starting the experiment, it was used in the cold trap with the continuous sampling bottle to reach the required temperature for the water condensation. To create the vacuum required for pervaporation on the permeate side, the vacuum pump was switched on. Using the needle valve, the vacuum pressure was adjusted to the required level.

The experiments were conducted in batch mode. For each experiment, weights of ethanol and distilled water were calculated. Next, water was weighed. Ethanol was weighed as well. The two components were mixed together since there was no reaction between them. The mixture of ethanol and water is then heated to the operating temperature and added to the reactor. At a desired feed rate, the mixture was continuously pumped through the pervaporation unit. This was the starting point of the experiment. The pumping rate may be set using a controller connected to the pump, and it is displayed in the LabVIEW program running on a personal computer. The reaction temperature was kept constant within ±10°C (the minimum temperature difference that can set in the heater) by using an oil heating bath.

Samples were taken from the glass reactor. The first sample was taken at the beginning of the experiment. The next two samples were taken 30 minutes apart. After that, all samples were taken one hour apart. The ability to collect spot samples from the permeate side was possible, but it was not taken since the amount of a spot sample obtained was too small to be analyzed with Raman spectroscopy. When such a sample size is available, GC could be used. However, due to its unavailability here, the method could not be used. Therefore, spot sampling was not conducted. In contrast, throughout the experiment, permeate was collected and used for analysis.

After the last sample was taken, the feeding pump was shut off. The polymer tubes between the glass reactor and membrane cell were disconnected from the membrane cell. The liquid in the tubes and in the membrane were collected. The vacuum pump was then turned off. This was done to prevent the membrane from soaking up liquid. The glass reactor was emptied and cleaned thoroughly. The continuous sample bottle was disconnected and covered with a lid until the ice on the wall defrosted.

4.2.3 Analyses

Samples collected from the feed side and the permeate side were analyzed to determine the compositions of the mixtures. Raman spectroscopy was used for the analysis and Raman Rxn2 analyzer from Endress+Hauser Group Services AG used as the analyzer. Apart from that permeate was weighed to calculate the fluxes. The sample analysis by Raman Rxn2 analyzer is shown in Figure 4.6.

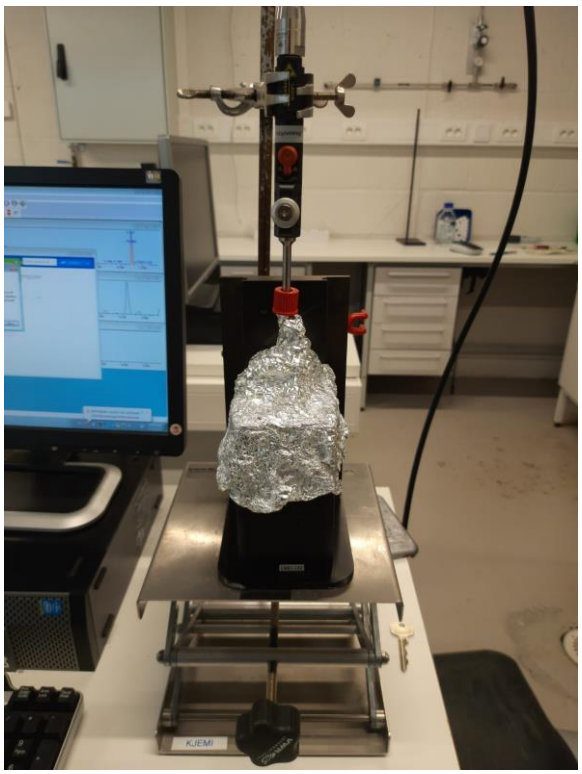

Figure 4.6: Sample analysis by Raman Rxn2 analyzer.

One of the main reasons to switch from esterification experiments to ethanol water mixture experiments was the unavailability of separate peaks for each component in the Raman spectrogram specially for ethanol and water. The Figure 4.7 shows the Raman spectrograms of ethanol, acetic acid, water, and ethyl acetate in the same graph. The peaks above 2000cm^{-1} wavenumber were useless since they were all overlapping each other in here. Thus, the wavenumber below 2000cm^{-1} was used to find peaks for the creation of a calibration curve and the determination of sample composition. Figure 4.8 shows the Raman spectrograms of pure components of ethanol, acetic acid, water and ethyl acetate below the wavenumber 2000cm^{-1}.

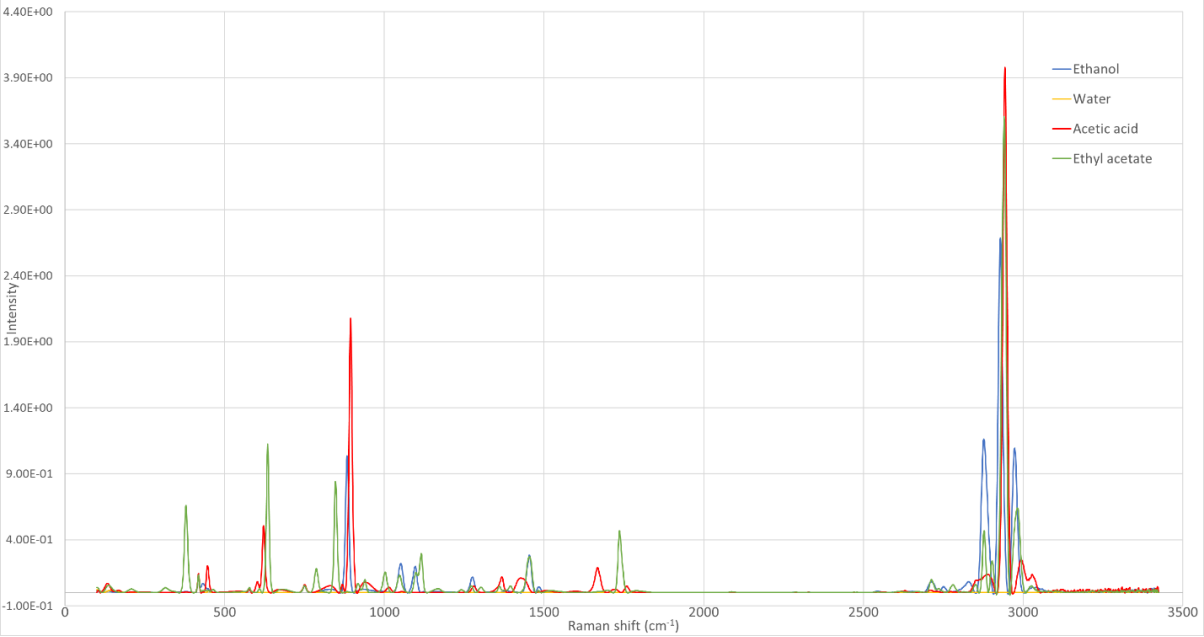

Figure 4.7: Raman spectrograms of pure components of ethanol, acetic acid, water and ethyl acetate.

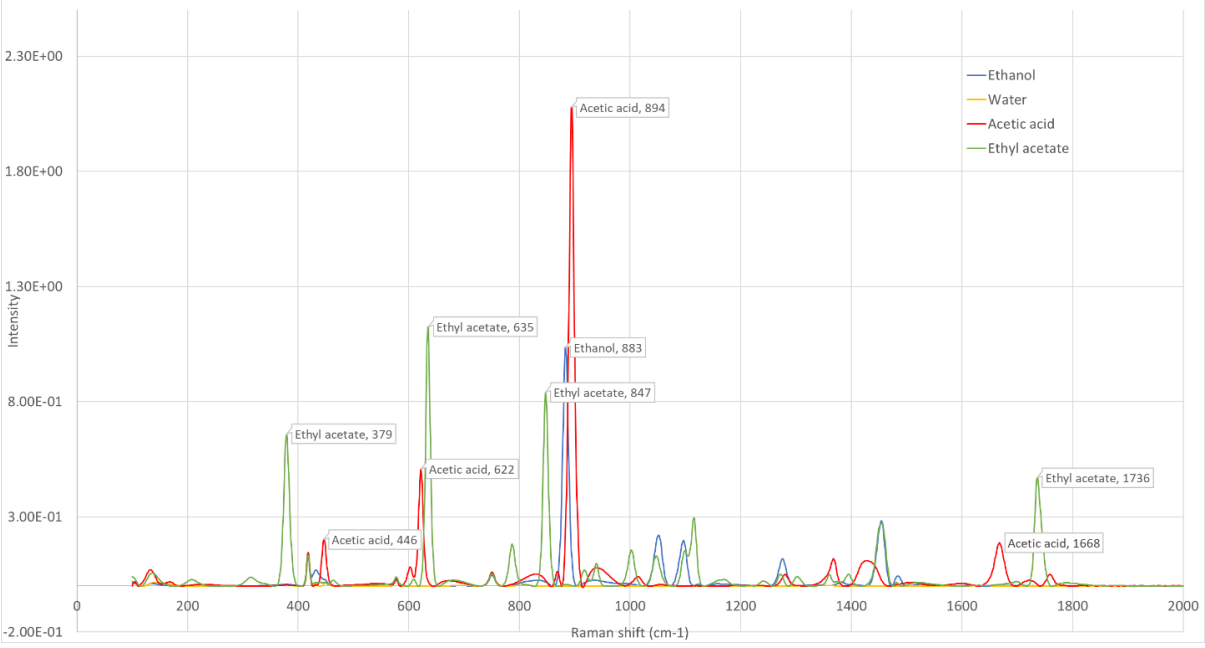

Figure 4.8: Raman spectrograms of pure components of ethanol, acetic acid, water and ethyl acetate below the wavenumber 2000cm^{-1}.

Figure 4.8 shows that for one component, several peaks can be taken. Some of the peaks are isolated, while others overlap. Peaks that overlap cannot be used. Large, isolated peaks are best for analysis. Hence, the Table 4.2 below gives the wavenumbers of the peaks that can be used for analysis.

Table 4.2: Wavenumbers of the peaks that can be used for analysis.

Component	Wavenumbers that could be used (cm^{-1})
Ethanol	883
Acetic acid	894, 622, 446, 1668
Ethyl acetate	635, 847, 379, 1733
Water	-

Based on the Table 4.2, only one peak for ethanol (blue curve in Figure 4.8) could be taken (at 883cm^{-1}), and even that peak partially overlaps. As for acetic acid (red curve in Figure 4.8), four peaks could be identified. However, even here, the first largest peak (at 894cm^{-1}) and the second largest peak (at 622cm^{-1}) partially overlap with other peaks. Nevertheless, one clear peak can be seen here (at 1668cm^{-1}) without any overlap. In the case of water (yellow curve in Figure 4.8) no peaks could be seen without overlapping. For ethyl acetate (green curve in Figure 4.8), one peak (at 379cm^{-1}) could be seen without any overlap.

For analysis, a known compound mixture (ethanol 12.5%, acetic acid 62.5%, ethyl acetate 12.5% and water 12.5% on weight basis) was taken and a Raman spectrogram (black curve in Figure 4.9) was obtained. Figure 4.9 illustrates it.

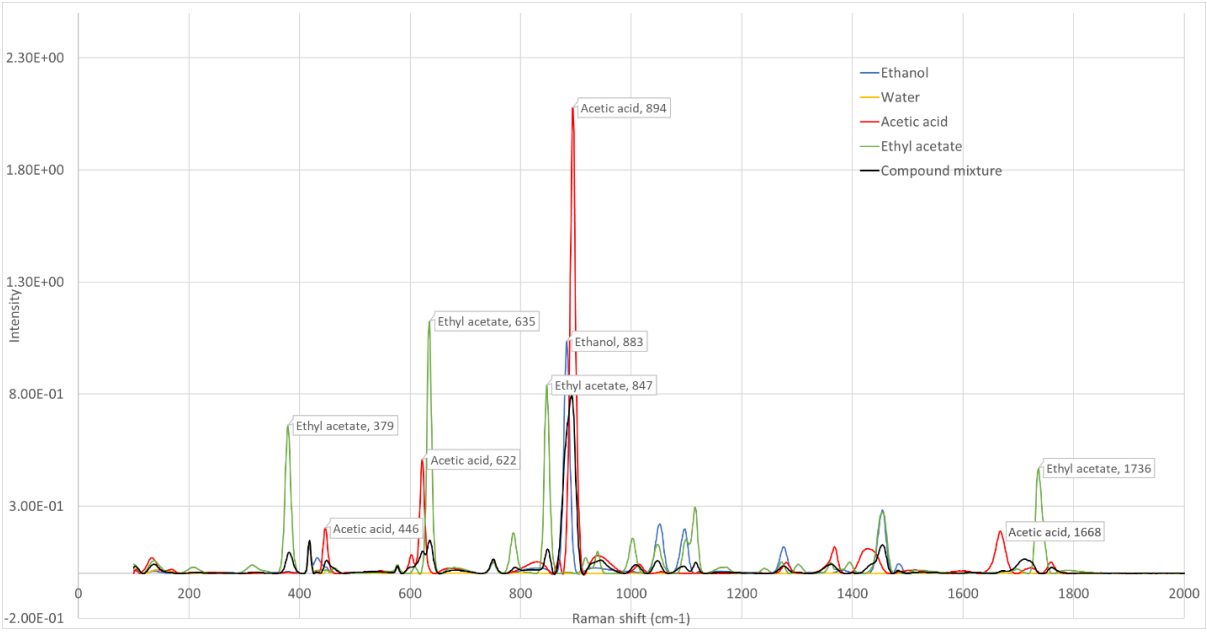

Figure 4.9: Raman spectrograms of pure components of ethanol, acetic acid, water, ethyl acetate and compound mixture (ethanol 12.5%, acetic acid 62.5%, ethyl acetate 12.5% and water 12.5% on weight basis).

In the spectrogram for the mixture, some of the peaks that were partially overlapping are now shown as one peak. Consequently, the component fraction cannot be determined. Ethanol

peak at 883cm^{-1} and the acetic acid peak at 894cm^{-1}, could not be distinguished from each other in the mixture. As the only peak available for ethanol is now unavailable, the fraction of ethanol cannot be determined.

Thus, Raman spectroscopy could not be used to determine the composition for the esterification reaction used in this study. Gas chromatography is another option for quantifying the fractions of each component. Unfortunately, the GC measurements were not possible due to its unavailability. Thus, the esterification reaction could not be assessed. Hence, the switch to ethanol water mixture experiments from esterification experiments.

A calibration curve should be used to measure the ethanol fraction in a sample. Raman spectrograms of several known ethanol water mixtures could be used to draw the calibration curve. Table 4.3 below shows the known mixtures, the Raman spectra intensities and the wavenumbers chosen.

Table 4.3: Raman spectra intensities and the wavenumbers chosen for known ethanol water mixtures.

Ethanol water mixture composition approximately	Ethanol		
	w/w %	Intensity	Wavenumber(cm^{-1})
Ethanol 0% and water 100%	0	1.28E-04	879
Ethanol 5% and water 95%	5.0536	9.61E-02	879
Ethanol 10% and water 90%	10.0518	1.93E-01	879
Ethanol 15% and water 85%	15.1075	2.87E-01	879
Ethanol 20% and water 80%	19.7775	3.72E-01	879
Ethanol 25% and water 75%	25.0315	4.69E-01	879
Ethanol 50% and water 50%	50.0597	8.56E-01	881
Ethanol 75% and water 25%	7.50E+01	1.27E+00	882
Ethanol 85% and water 15%	8.43E+01	1.41E+00	882
Ethanol 90% and water 10%	9.00E+01	1.50E+00	883
Ethanol 95% and water 5%	9.50E+01	1.57E+00	883
Ethanol 100% and water 0%	9.99E+01	1.63E+00	883

In this case, several wavenumbers were used to obtain the intensity value from the Raman spectrogram. This is mainly due to the peak shift that can be seen in the Raman spectrograms for each mixture (even though the sample temperatures were same). From previous

experience of people who worked with the instrument, a ± 5 cm^{-1} variation in the shift can be seen for a particular sample mixture with varying concentrations. Raman spectrograms are shown in Figure 4.10 for each known mixture of ethanol and water.

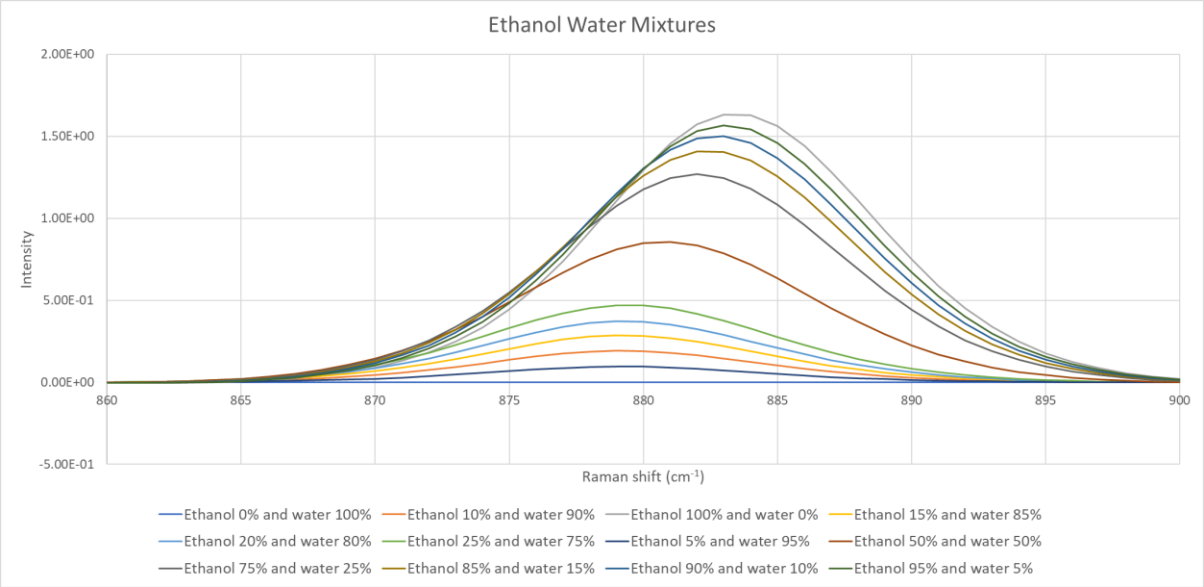

Figure 4.10: Raman spectrograms for known mixture of ethanol and water between wavenumbers 860cm^{-1} and 900cm^{-1}.

Due to this shift in the peaks, the wavenumber that should be taken for a composition range has been determined. It has been done in order to determine the maximum intensity of the peak. The Table 4.4 shows the defined composition ranges and their corresponding wavenumbers.

Table 4.4: Defined composition ranges and corresponding wavenumbers.

Composition range for ethanol %	Wavenumber (cm^{-1})
$100 \geq x > 85$	883
$85 \geq x > 65$	882
$65 \geq x > 45$	881
$45 \geq x > 25$	880
$25 \geq x > 0$	879

From the intensity values, calibration curve was made. The calibration curve for ethanol water mixtures, drawn from the data in Table 4.3 is given below (Figure 4.11).

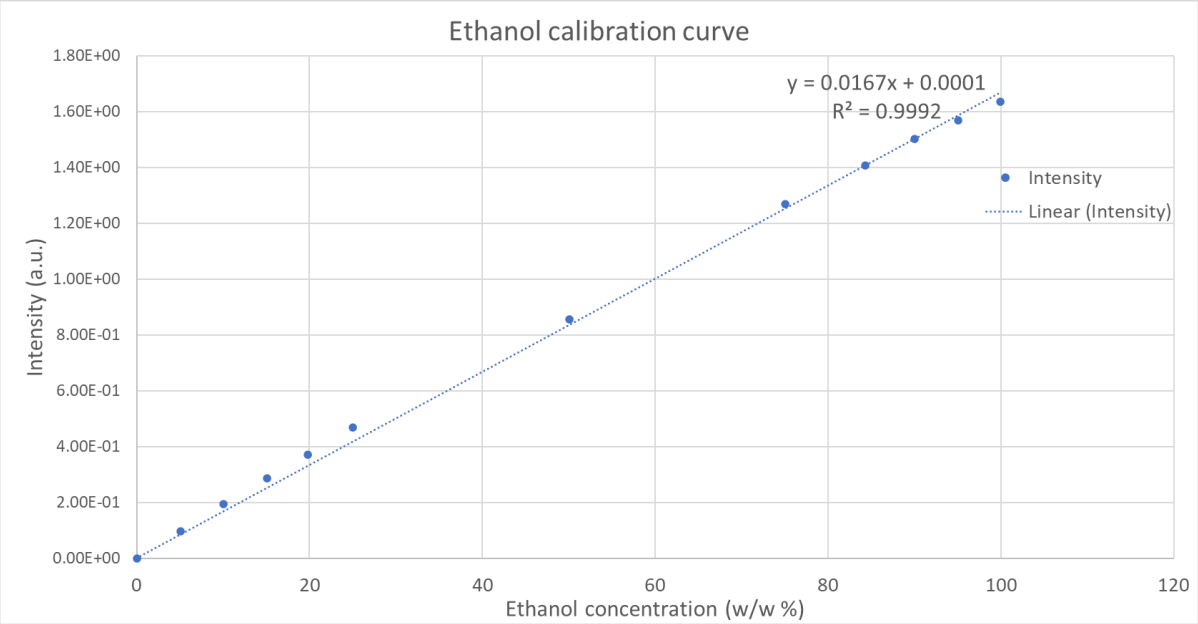

Figure 4.11: Calibration curve for ethanol water mixtures.

A linear regression line for the data points were made in Microsoft Excel and the equation for that is given below (Equation 4.1).

$$y = 0.0167x + 0.0001 \tag{4.1}$$

In here y is the intensity (arbitrary unit) and the x is the weight fraction percentage (w/w %). In this way, it would be possible to measure the composition of an ethanol water sample. It is worth noting that an intensity value existed for the sample with 0 % ethanol concentration (only distilled water). Therefore, that intensity value was used as the intercept for the linear regression line, leading to the above equation.

4.2.4 Experiments plan

Due to the unexpected time spent on the construction of the setup, unexpected breakdowns in the system during experiments, and the unavailability of the required analytical method to test the samples, the experiment plan had to be revised. During this limited period, the following factors were studied through experiments:

- The membrane behavior with varying temperatures.
- Effects of varying initial feed concentration on separation.
- Study of various membranes behavior for same parameters.

Table 4.5 shows the revised experiment plan. The previous plan for the esterification experiments has been attached in appendix A.

Table 4.5: Revised experiment plan.

Experiment	Membrane	Temperature (^{o}C) (Feed and membrane cell)	Initial water concentration in feed (w/w %)
1	PERVAP™ 4100	70	15
2		70	25
3		70	35
4		60	35
5		80	35
6	PERVAP™ 4101	70	15
7		70	25
8		70	35
9		60	35
10		80	35

However, a sudden failure of the feeding pump during an experiment led to an abrupt end to the experiments, so the PERVAP™ 4101 could not be tested. Other experimental parameters are shown in Table 4.6.

Table 4.6: Other experimental parameters.

Parameter	Value
Run time	4 hours
Feed rate	0.5 l/min
Vacuum pressure	10 mbar
Initial feed volume	500 ml
Membrane area	155 cm^2
Ice-salt mixture temperature	-13 ^{o}C
Membrane cell holder pressure	100psi

5 Results and Discussion

In this chapter, experimental results and the challenges faced during construction of experimental setup and during experiments are explained and analyzed.

5.1 Experimental results and discussion

5.1.1 Effects of varying initial water concentration in feed

The initial water concentration was varied in these experiments. The temperature was maintained at 70^{o}C. In this case, the temperature was chosen so that the water-ethanol mixture would not boil at the membrane feeding end. The approximate boiling points of ethanol water mixtures at atmospheric pressure are given below [88]. (Table 5.1)

Table 5.1: Approximate boiling points of ethanol water mixtures at atmospheric pressure.

Ethanol concentration (w/w %)	Boiling Point (^{o}C)
85	78.38
75	79.25
65	80.38

Using the Raman spectroscopy, the intensities for each sample were determined and the ethanol concentration was calculated from the calibration curve. Figure 5.1 shows the ethanol concentration versus time curves for each starting concentration.

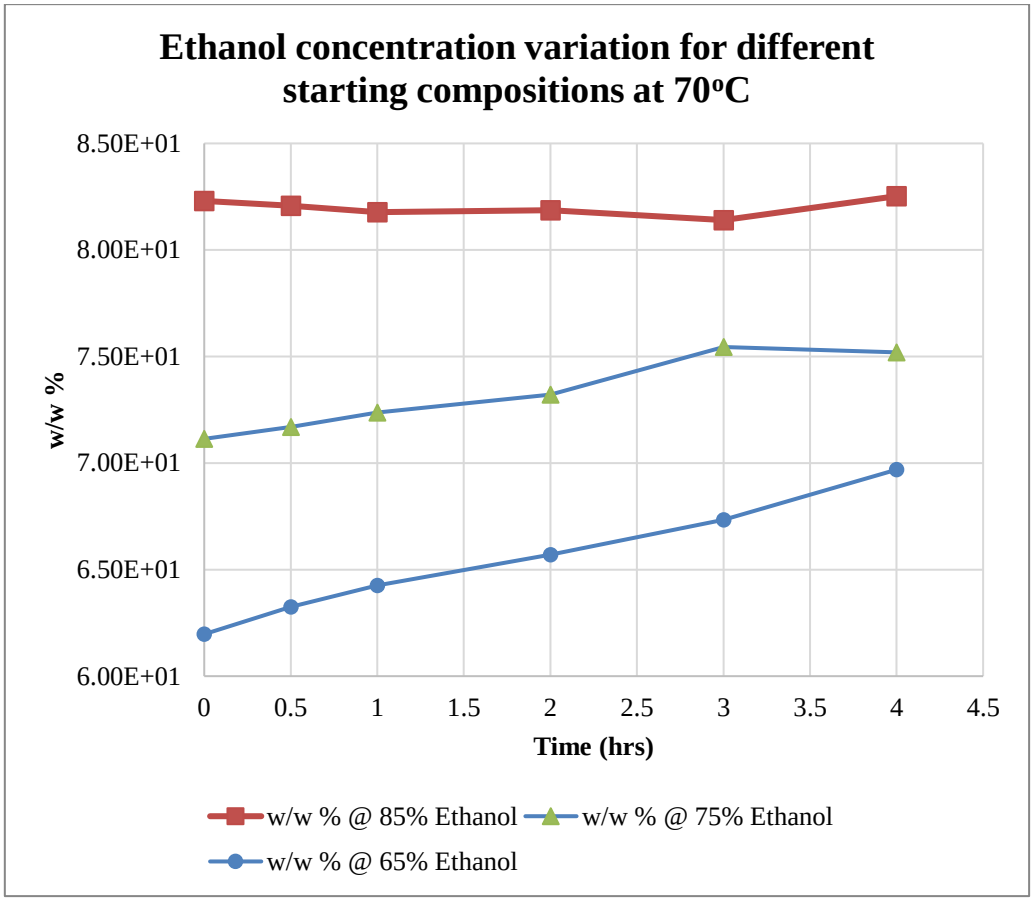

Figure 5.1: Ethanol concentration versus time curves for each starting concentration.

Although the starting composition is mentioned in Table 5.1 above, values at Time (T) = 0 are less than the starting concentration. Ethanol is a highly evaporative liquid. Therefore, after preheating, there was a reduction in feed concentration due to the evaporation during the feed addition to the glass reactor. For this reason, the concentration at T= 0 should be used as the starting concentration. The reduction of ethanol in the feed increased the boiling point, thereby reducing evaporation tendency at 70°C.

The new starting concentrations are shown in Table 5.2 and these were used in calculations

Table 5.2: Starting concentrations of ethanol at T = 0.

Initial concentration (w/w %)	Ethanol concentration at T = 0 (w/w %)
85	82.3
75	70.9
65	61.5

Raman spectroscopy was performed on the permeate collected during the experiment to identify the sample composition and determine the separation factor. The permeate flux was also calculated by weighing the permeate. The Table 5.3 shows the permeate fluxes, feed and permeate component compositions as well as the separation factors for varying initial water concentrations in feed.

Table 5.3: Permeate fluxes, feed and permeate component compositions and the separation factors for varying initial water concentrations in feed.

Initial concentration (w/w %)	Fluxes (kg m^{-2} h^{-1})			Feed concentration at T = 0 (w/w %)		Permeate concentration (w/w %)		Separation Factor (β)
	Total	Ethanol	Water	Ethanol	Water	Ethanol	Water	
85	2.01E-01	4.18E-03	1.97E-01	82.3	17.7	2.08	97.9	218.8
75	3.89E-01	1.52E-02	3.74E-01	71.1	28.9	3.90	96.1	60.7
65	7.71E-01	1.73E-02	7.53E-01	62.0	38.0	2.25	97.7	70.8

These data are given graphically in Figure 5.2 and Figure 5.3 below.

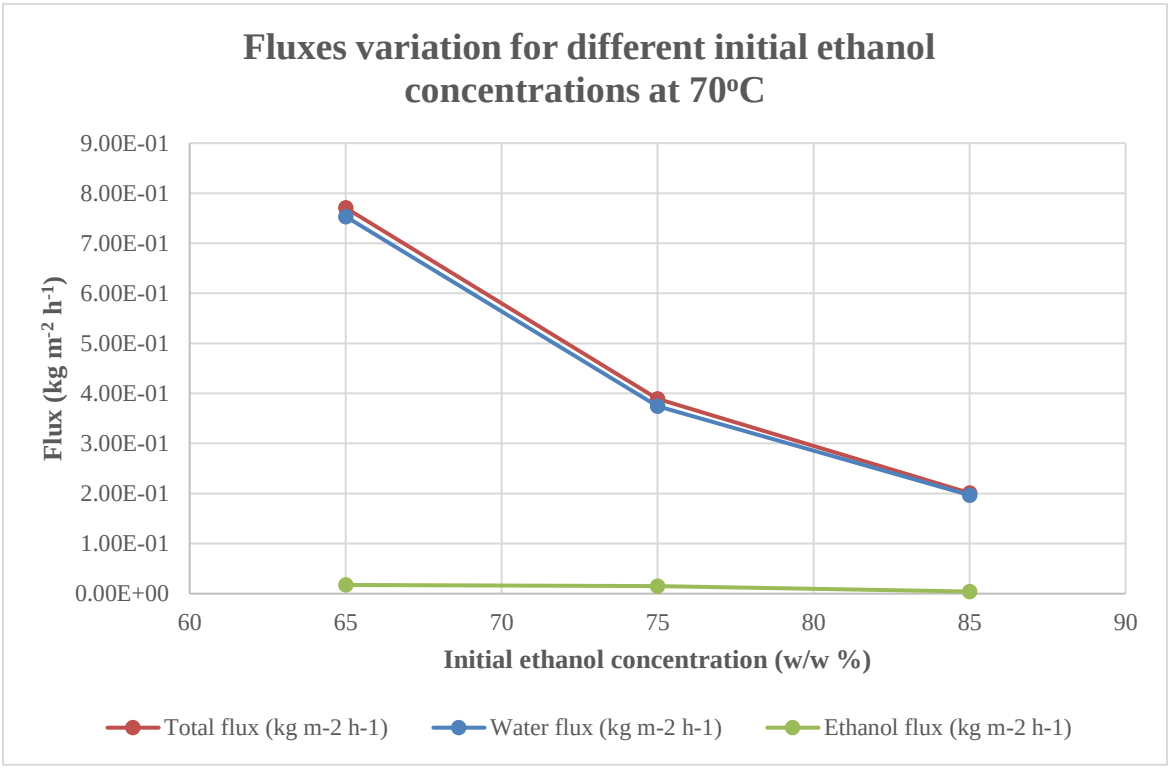

Figure 5.2: Fluxes variation for different initial ethanol concentrations at 70°C

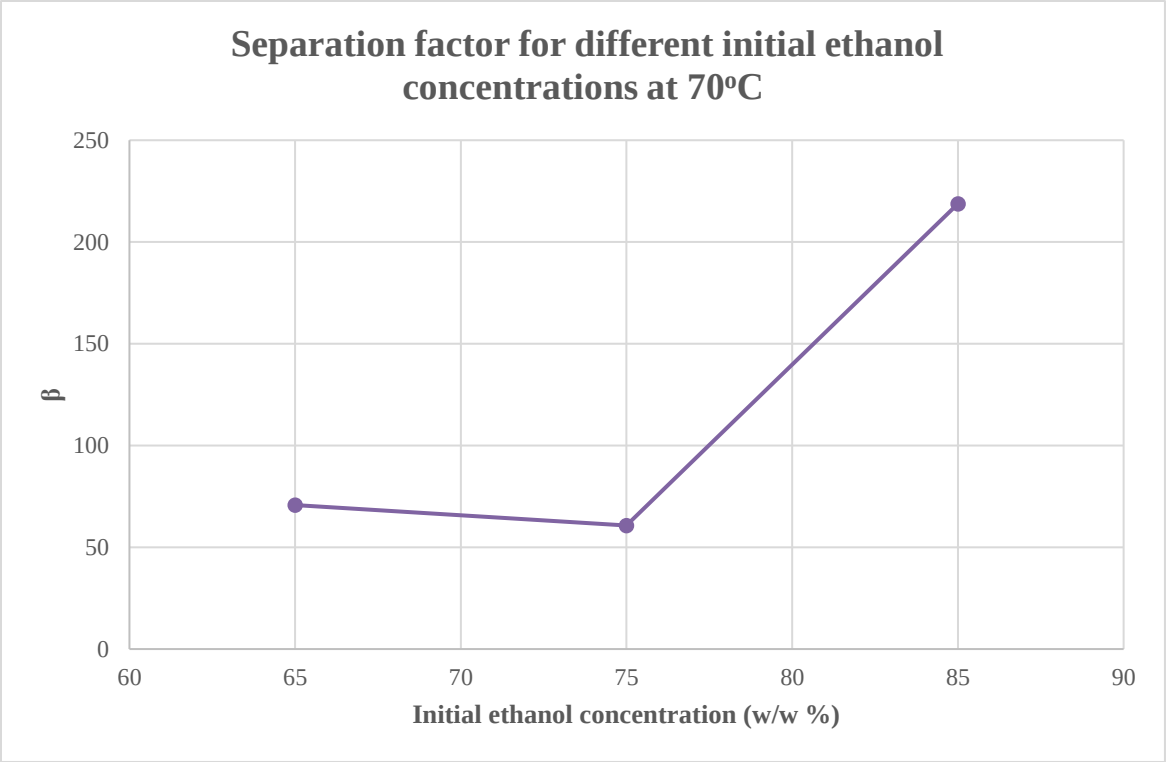

Figure 5.3: Separation factor for different initial ethanol concentrations at 70°C.

These results indicate water concentrations are always higher than the corresponding feed concentrations. As the water concentration in feed increases, the separation factor decreases. In the separation of high concentration aqueous solutions of ethanol through the membrane, high separation factors can be obtained. Water flux increases almost proportionally to the water concentration in the feed, while ethanol flux is almost constant regardless of the feed composition.

In cases where the feed contains more water, the degree of swelling is high in the membrane. The result is higher water flux through the membrane due to higher water permeance. Furthermore, increased swelling promotes fractional free volume in the membrane, thus increasing the amount of ethanol permeating through it. This explains the reduced separation factor with increased water concentration in the feed. Due to this, the mixture for this membrane should have a lower water content in order to have a better separation.

It should be noted that since only the ethanol concentration values were obtained from Raman spectroscopy, the water concentration values were obtained by subtracting the ethanol concentration from 100%. It was possible to do so here since the mixture is dual component. However, this is not possible for the esterification reactions. The Karl Fischer titration can be used for quickly and precisely determining the water content. For feed side samples, gas chromatography could provide a more precise quantitative composition analysis.

5.1.2 Effects of varying operating temperature

In these experiments, the operating temperature was varied while the other parameters were kept constant. As it is already explained in the previous section, the initial concentration was taken as the concentration at T = 0. For all three experiments, the concentration reduction is almost the same due to evaporation during feed loading to the glass reactor. Because the concentration at the start is roughly the same (62% - 64%), comparisons of these mixtures can be made.

The same procedure was used to determine the ethanol concentration of each sample. Figure 5.4 illustrates the concentration versus time curves for each temperature.

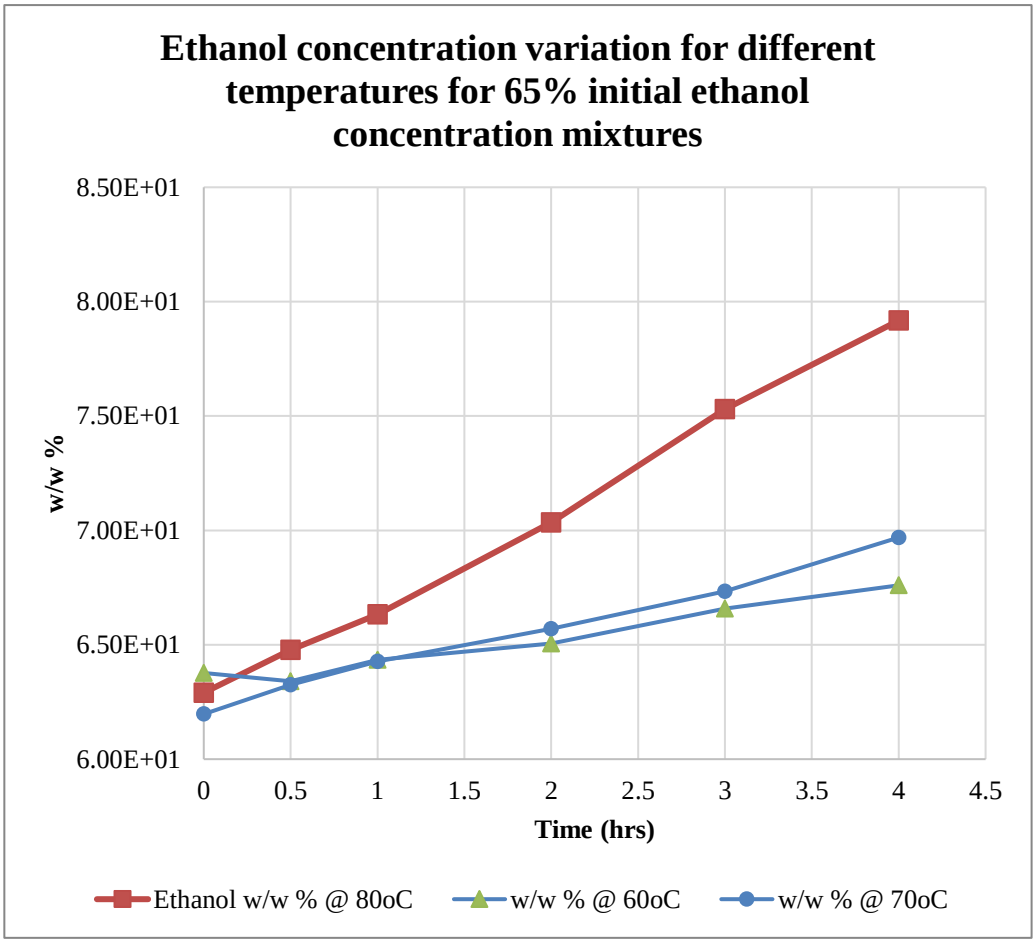

Figure 5.4: Ethanol concentration variation for different temperatures for 65% initial ethanol concentration mixtures.

Table 5.4 shows the permeate fluxes, feed and permeate component compositions as well as the separation factors for varying temperatures.

Table 5.4: Permeate fluxes, feed and permeate component compositions and the separation factors for varying temperatures.

Temperature (°C)	Fluxes (kg m^{-2} h^{-1})			Feed concentration at T = 0 (w/w %)		Permeate concentration (w/w %)		Separation Factor (β)
	Total	Ethanol	Water	Ethanol	Water	Ethanol	Water	
80	1.41E+00	7.75E-02	1.34E+00	62.9	37.1	5.48	94.5	29.3
70	7.71E-01	1.73E-02	7.53E-01	62.0	38.0	2.25	97.7	70.8
60	6.33E-01	3.35E-02	5.99E-01	63.8	36.2	5.29	94.7	31.5

This is also shown graphically in Figure 5.5 and Figure 5.6 below.

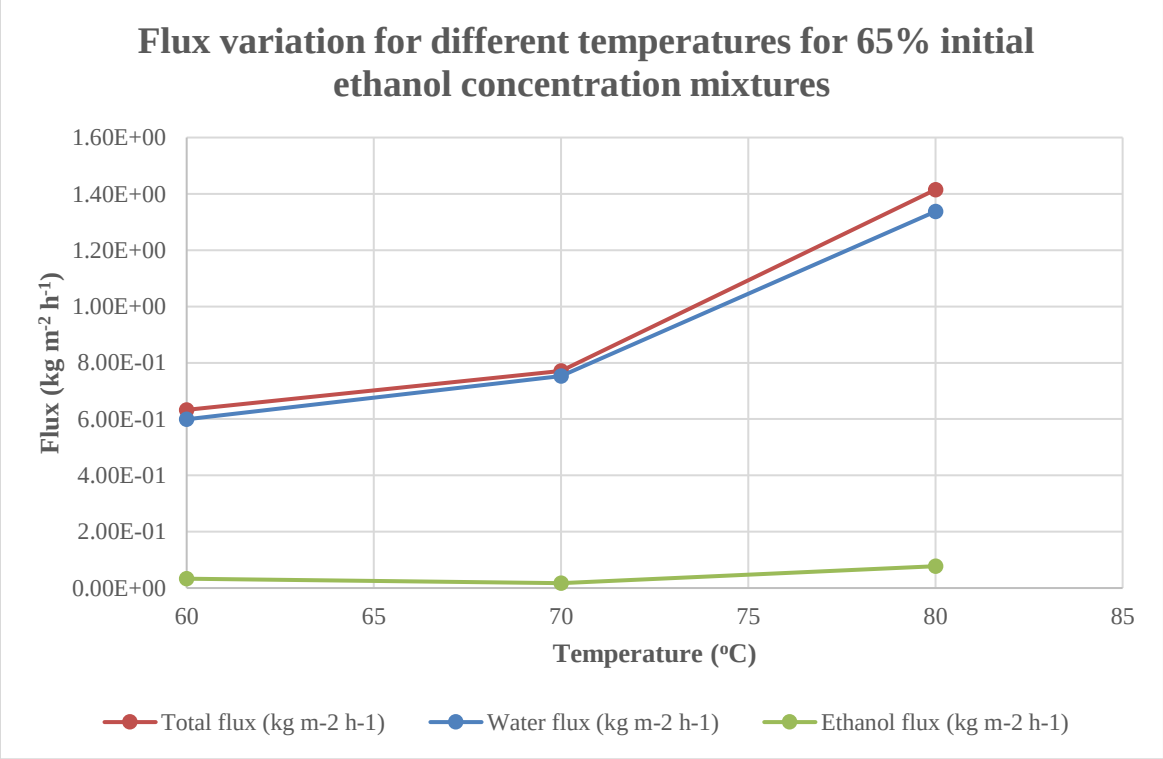

Figure 5.5: Flux variation for different temperatures for 65% initial ethanol concentration mixtures.

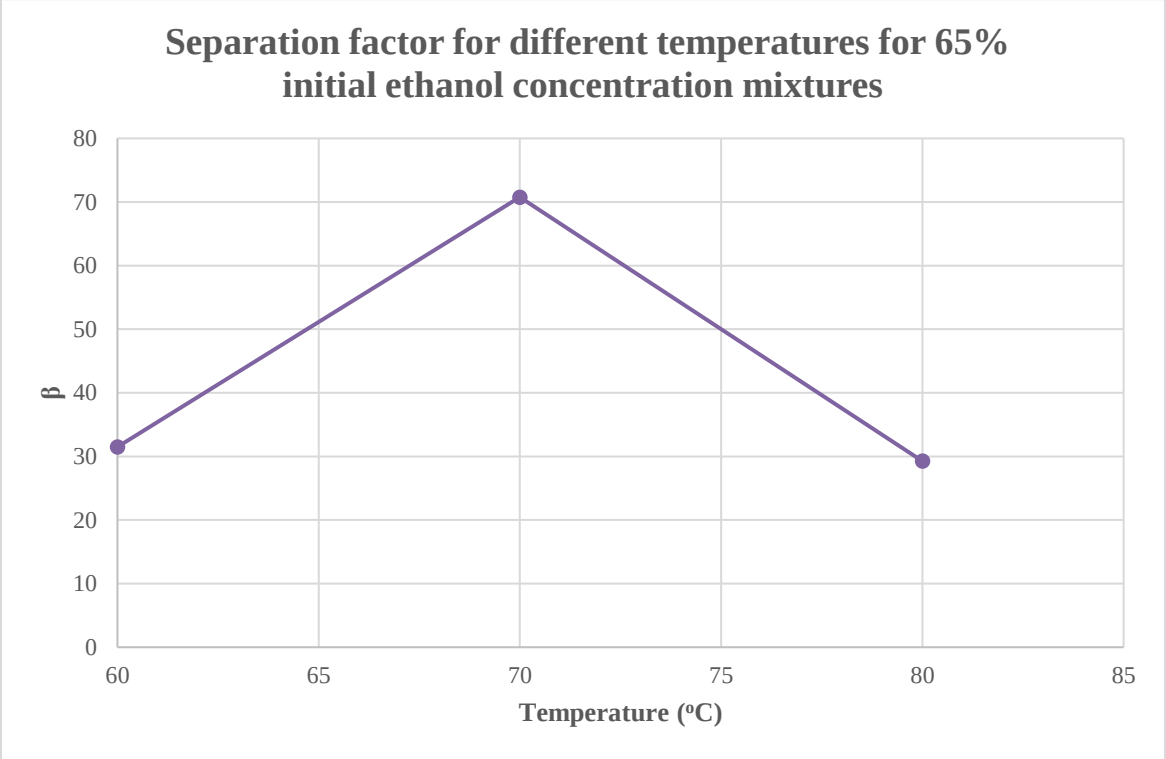

Figure 5.6: Separation factor for different temperatures for 65% initial ethanol concentration mixtures.

The effect of temperature on separation performance depends on two factors

- The temperature effect on the membrane material.
- The temperature effect on partial vapor pressure of the mixture components.

A temperature change will change the polymer chain mobility and the free volume in the polymer matrix and will lead to a change of solubility and diffusion of components through the membrane. In the glassy state ($T < T_g$) the free volume fraction remains almost the same[16]. However, after exceeding the glass transition temperature the free volume generally increases linearly[16]. In here, with increasing temperature, flux has risen indicating the membrane operating above glass transition temperature. Therefore, free volume increases with increasing temperature. Hence the increase of water flux almost proportionally with temperature, through the membrane.

Secondly, when the temperature changes, the partial vapor pressures of components will change[16]. Thus, the driving force changes since the vacuum pressure kept constant. In practice, to decrease the membrane area, high temperatures are preferred. However, this will increase the heating costs and have an impact on the thermal stability.

As for the separation factor, a clear conclusion cannot be derived since the variation of separation factor is not consistent with temperature.

For both types of experiments, it is recommended to do tests for several more concentrations as well as temperatures to derive more accurate conclusions. Several tests per each experiment will also contribute to accurate results since the calculations are not based solely on one experiment. Results could be compared and could omit erroneous results.

5.2 Challenges during setup construction and experiments

In this section, challenges encountered during setup construction and during experiments are presented. These reasons consumed most of the time available for the project delaying experiments to be conducted

5.2.1 Ice-salt mixture preparation

Condensing the permeate coming from the membrane cell was one of the main challenges at the beginning. Cold traps and cooling methods were needed for this purpose. At 10 mbars, assuming the membrane cell permeate largely consists of water, the condensing temperature was 6.8^{o}C [89]. Despite being higher than the ice temperature, the gas phase permeate mixture should still condense quickly. If not, the mixture will be lost through the vacuum pump. In this case, the freezing point of the water at 10 mbar was also important. This is because the sampling bottles have narrow glass inlets into them. Therefore, the incoming gas should not freeze inside the glass tube and block the permeate coming from the membrane cell. This can also increase the permeate side vacuum in the membrane cell, which is not desirable in these experiments. At 10 mbars, water has a freezing point of 0^{o}C [90]. In order to allow the permeate to condense as quickly as possible, the temperature inside the glass tube should be between 6.8^{o}C and 0^{o}C and the temperature in the bottle should be at minus degrees Celsius. Condensate freezing on the sampling bottle is not a problem since it does not interfere with the experiment. However, there was a waiting time before collecting the permeate from the continuous sampling bottle.

In this case, the cheapest method would be to use ice and salt (NaCl) mixture, which can reach -21^{o}C for a weight ratio of 3:1 of ice to salt. During preliminary testing with this ice salt mixture, it was observed that the water froze inside the glass tube of the sample, impairing the flow of the permeate to the sample bottle. This led to the need for a mixture of salt water that could provide a higher temperature. Through several trials, a mixture was found that allowed proper cooling without causing water to freeze inside the glass tube in the sampling bottle, while some water froze on the wall of the bottle. The ice-salt weight ratio was 1:9 and the maximum negative temperature reached was -13^{o}C.

A second important observation was that the sampling bottle should be submerged up to the neck of the sampling bottle. Otherwise, the vacuum grease applied to the neck could solidify, resulting in the loss of vacuum within the bottle.

5.2.2 Sampling system challenges

10mbar was the lowest direct measurement of the vacuum pressure gauge used. Therefore, the vacuum pressure that could be applied to the system was limited to 10mbar where an indication could be taken from the pressure gauge. Fortunately, this pressure was sufficient for the application. However, a pressure gauge with a higher resolution might be useful when setting the pressure accurately for the permeate side. The setup shown in the experimental setup construction section, was not the setup built at the initial stage of the project. New setup had to be built with a longer permeate carrier line to the samples. This line has both advantages and disadvantages. Since this is exposed to the atmosphere, the permeate temperature can drop, which will reduce both the heat required and the heat transfer rate required for the permeate to condense. However, the pressure drop is high since the tubing is longer. It is a disadvantage. As a result, the pressure in the sample bottle can differ from the

pressure in the permeate side. With shorter line, this deviation is small, so one pressure gauge is sufficient.

Another challenge was finding a proper spot sampling method. Because the spots samples are taken over a short period of time, a small bottle should suffice. It was difficult to find a cold trap that fit the height of the sampling bottles. A shorter one was found. To have a sufficient heat transfer, the sampling bottle had to be submerged up to its neck. Therefore, the cold trap was modified with cardboard, aluminum foil, and insulation material that was available in the lab, in order to meet the required height. It was necessary to modify the spot sampling bottle itself so that it could connect to the sampling system. To incorporate inlet and outlet tubes to the bottle, a lid was drilled. With this method, the spot sample is taken directly to a small sample bottle used for analysis. Since the spot sample bottle could be easily replaced with another one, the need for liquid transfer and spot sample bottle cleaning before collecting the next sample was eliminated.

5.2.3 Feed pump issues

Initially, a 12W centrifugal feed pump was used. However, its efficiency decreased over time during the experiment. Therefore, power to the pump should be increased with the controller to maintain a constant feeding rate. However, the maximum feed rate the pump is capable of delivering plummets dramatically, and the required feed rate cannot be achieved by the pump. Therefore, new pump with 24W power rating had to be utilized for the feed pumping.

Since this is a centrifugal pump, bubbles can reduce the efficiency of the pump. From time to time, the bubbles accumulated in the impeller section had to be removed by changing the orientation of the pump, so that they could escape through the discharge. Bubbles in the feeding system occur because of splashing in the glass reactor caused by the retentate entering the reactor. The splashes occur near the inlet of the glass tube that supplies the pump with feed. As a result, the bubbles formed entered the glass tube through the inlet. This can be solved by bending the glass tube and taking the feed from different locations within the reactor.

Finally, the pump began leaking during an experiment, causing the experiment to be stopped. A replacement pump should be found and used with appropriate connections and tubes. The experiment could not be continued because of limited time hence the experimentation brought to an end.

5.2.4 Flow meter calibration

The flow meter must be calibrated before it can be used. With Fredrik's help, a LabVIEW program was also developed in order to calculate the flow rate from the signals received from the magnetic turbine flow meter, and to display the calculated flow rate continuously. Depending on the flow rate range of the experiments, a nozzle could be placed inside the meter. Thus, an appropriate nozzle for 0.5l/min feeding was inserted into the flow meter. Next, it was calibrated and tested. Water was pumped through a flowmeter and collected in a measuring beaker to determine the flow rate. Based on that, the time taken to reach a certain volume was measured and the flow rate calculated. The flow rate was constant during this period, and the flow rate displayed in LabVIEW was compared to the actual flow rate. When the displayed flow rate doesn't match the actual flow rate, the software can be adjusted to show the correct flow rate. The piping system in this testing setup mimicked the piping

system in the actual experiment setup, so the system would experience about the same pressure drop as the experimental setup.

5.2.5 Issues in the compressed air supply to the PVR

The compressed air system had approximately 100psi pressure at the pressure outlet. Since a reinforced hose was used to supply the compressed air to the membrane holder, the connection mechanism was problematic. Several methods were utilized to connect the hose to the holder. But these methods could not hold the pressure present in the compressed air system. However, direct connection to the threaded shutoff valve with clamps worked and used in the experiments.

Initially, the experimental setup did not include an oven. Therefore, the tubing purchased for the compressed air supply to the PVR was perfectly adequate to meet the requirements of the system. However, when the setup was tested, the temperature could not be maintained at the required operating level. The main cause for this is the dissipation of heat from the membrane cell. The membrane cell is a giant block of steel, so it is an efficient heat conductor. To solve this problem, the membrane cell was placed in an oven. Generally, the oven temperature in these experiments was kept 20^{o}C higher than the operating temperature. This allowed the membrane cell to operate at its set temperature. As a result of these high oven temperatures, the reinforced PVC hose became weakened due to its increased flexibility. As a consequence, constant breakdowns occurred. To remove the weakened hose part, a piece of hose was cut and removed. A simple solution would be to use metal piping to supply compressed air.

6 Conclusion

Constructing an experimental setup was a tedious process that took a lot of time and patience. Regardless, the project will provide valuable information for upcoming work on CO_2 utilization in ester formation using pervaporation technology. Experience gained during the experiment could be utilized in the future to purchase material for the setup, build an improved version of the setup, develop procedures for future experiments, choose operating conditions, and conduct experiments at the experimental setup.

The glass reactor system should be designed to hold a sufficient amount of liquid and enable easy sampling. It should also be capable of handling the operating temperatures. The piping should be able to handle the temperatures, pressures, and liquid and vapor materials flowing through it during the experiment. The PVR holder should have a sufficient amount of air supply through tubes with adequate pressure and temperature ratings. The feeding pump should be chosen carefully to fit the system with the appropriate power rating to provide the required fluid flows, as well as temperature rating to handle the temperatures in the feeding fluid. The vacuum pump is an integral part of the pervaporation process. Therefore, the use of a powerful vacuum pump provides a higher driving force through the membrane. Having an appropriate sampling system is one of the highest priorities since all analyses are based on samples collected during experiments. In order to get accurate results, it is necessary to use the correct analytical methods. Temperature and pressure indicators play a key role as well. Especially the vacuum pressure indicator should be capable of indicating low pressures (1mbar - 20mbar), which have a great impact on experiments. In experiments, the cooling of permeate in cold traps plays a major role as well.

As for the experiments, for polymeric pervaporation membrane (PERVAPTM 4100) that swell [91], it could be demonstrated that flux and separation factor are dependent on operating temperature as well as the initial water/ethanol concentration in the feed. For higher water concentrations in the feed higher total fluxes could be taken from the permeate side. However, the separation factor decreases with increased water concentration. With increasing temperatures, higher total flux could be taken from the permeate side. However, a clear conclusion could not be derived from the separation factor for varying temperatures.

Overall, the experimental setup could be used for pervaporation and above 94% water concentration could be achieved in permeate side for the temperature-varying experiments while a water concentration of 96% or above could be achieved in permeate side for varying initial ethanol concentrations.

7 Further work

The experimental setup could be improved by a number of modifications. Among them are,

- For compressed air delivery to the membrane holder, use metal tubing that can withstand the high pressure and temperature resulting in fewer breakdowns.
- Feed reactors should have easy access for sampling.
- Preheating mechanism for components connected to feed reactor to prevent loss of components through evaporation during preheating and loading.
- Cooling system for cold traps to eliminate preparation and manual loading of ice salt mixture.
- Better operating parameter indicating and controlling mechanism.
- Use of a diaphragm pump with dampener instead of a centrifugal pump in order to prevent priming of the pump and problems caused by bubbles.
- Retentate supply directly into the liquid to avoid bubble formation due to splashing.

In addition to these modifications, experimental setups other than the configuration utilized should also be studied, such as catalytic pervaporation membrane reactors, in situ separation units, semi-batch tank reactors with separation units, tubular reactors with separation units, etc.

To provide a more comprehensive analysis for varying temperatures and initial concentrations, additional experiments need to be conducted with the membrane. In particular for the temperatures at which ethanol evaporates, testing should be done to determine the permeance of the feed mixture consists of liquid (mostly water) and vapor (mostly ethanol).

References

[1] H. Hart, C. M. Hadad, L. E. Craine, and D. J. Hart, *Organic chemistry: a short course*, 13th ed. Cengage Learning, 2011.

[2] S. Hari Krishna and N. G. Karanth, "Response Surface Modeling of Lipase-Catalyzed Isoamyl Propionate Synthesis," *Journal of food science*, vol. 67, no. 1, pp. 32-36, 2002, doi: 10.1111/j.1365-2621.2002.tb11354.x.

[3] M. C. Romano *et al.*, "Application of Advanced Technologies for CO2 Capture From Industrial Sources," *Energy Procedia*, vol. 37, pp. 7176-7185, 2013, doi: 10.1016/j.egypro.2013.06.655.

[4] M. Aresta, A. Dibenedetto, A. Angelini, and I. Pápai, "Reaction Mechanisms in the Direct Carboxylation of Alcohols for the Synthesis of Acyclic Carbonates," *Topics in catalysis*, vol. 58, no. 1, pp. 2-14, 2014, doi: 10.1007/s11244-014-0342-0.

[5] V. S. Chandane, A. P. Rathod, K. L. Wasewar, and S. S. Sonawane, "Esterification of propionic acid with isopropyl alcohol over ion exchange resins: Optimization and kinetics," *The Korean journal of chemical engineering*, vol. 34, no. 1, pp. 249-258, 2016, doi: 10.1007/s11814-016-0249-5.

[6] K. Liu, Z. Tong, L. Liu, and X. Feng, "Separation of organic compounds from water by pervaporation in the production of n-butyl acetate via esterification by reactive distillation," *Journal of membrane science*, vol. 256, no. 1, pp. 193-201, 2005, doi: 10.1016/j.memsci.2005.02.020.

[7] V. S. Chandane, A. P. Rathod, and K. L. Wasewar, "Pervaporation Reactor for Enhanced Esterification of Lactic Acid and Isobutyl Alcohol," *Chemical engineering & technology*, vol. 43, no. 2, pp. 282-288, 2020, doi: 10.1002/ceat.201900153.

[8] T. J. Schildhauer, F. Kapteijn, and J. A. Moulijn, "Reactive stripping in pilot scale monolith reactors—application to esterification," *Chemical engineering and processing*, vol. 44, no. 6, pp. 695-699, 2005, doi: 10.1016/j.cep.2003.09.012.

[9] K. C. d. S. Figueiredo, V. M. M. Salim, and C. P. Borges, "Synthesis and characterization of a catalytic membrane for pervaporation-assisted esterification reactors," *Catalysis today*, vol. 133, no. 1-4, pp. 809-814, 2008, doi: 10.1016/j.cattod.2007.12.088.

[10] M. Zhang, L. Chen, Z. Jiang, and J. Ma, "Effects of Dehydration Rate on the Yield of Ethyl Lactate in a Pervaporation-Assisted Esterification Process," *Industrial & engineering chemistry research*, vol. 54, no. 26, pp. 6669-6676, 2015, doi: 10.1021/acs.iecr.5b01199.

[11] J. Otera and J. Nishikido, *Esterification: methods, reactions, and applications*. John Wiley & Sons, 2009.

[12] F. S. Atalay, "Kinetics of the Esterification Reaction Between Ethanol and Acetic Acid," *Dev. Chem. Eng. Mineral Process*, vol. 2, no. 2-3, pp. 181-184, 1994, doi: 10.1002/apj.5500020210.

[13] H. Arnikar, T. Rao, and A. Bodhe, "A gas chromatographic study of the kinetics of the uncatalysed esterification of acetic acid by ethanol," *Journal of Chromatography A*, vol. 47, pp. 265-268, 1970, doi: 10.1016/0021-9673(70)80037-1.

[14] I. Mochida, Y. Anju, A. Kato, and T. Seiyama, "Elimination reactions on solid acid catalysts: II. Esterification of ethanol with acetic acid," *Journal of catalysis*, vol. 21, no. 3, pp. 263-269, 1971, doi: 10.1016/0021-9517(71)90145-X.

[15] C. Beula and P. S. T. Sai, "Kinetics of Esterification of Acetic Acid and Ethanol with a Homogeneous Acid Catalyst," *Indian chemical engineer (Calcutta, India : 1997)*, vol. 57, no. 2, pp. 177-196, 2015, doi: 10.1080/00194506.2014.975761.

[16] M. Mulder, *Basic Principles of Membrane Technology*, 2nd ed. Dordrecht: Dordrecht: Springer Netherlands, 1996.

[17] G. Jyoti, A. Keshav, and J. Anandkumar, "Review on Pervaporation: Theory, Membrane Performance, and Application to Intensification of Esterification Reaction," *Journal of engineering (Cairo, Egypt)*, vol. 2015, pp. 1-24, 2015, doi: 10.1155/2015/927068.

[18] K. Zhou, Q. G. Zhang, G. L. Han, A. M. Zhu, and Q. L. Liu, "Pervaporation of water–ethanol and methanol–MTBE mixtures using poly (vinyl alcohol)/cellulose acetate blended membranes," *Journal of membrane science*, vol. 448, pp. 93-101, 2013, doi: 10.1016/j.memsci.2013.08.005.

[19] P. Larkin, *Infrared and Raman Spectroscopy: Principles and Spectral Interpretation*. Saint Louis: Saint Louis: Elsevier, 2011.

[20] K. H. Liland, A. Kohler, and N. K. Afseth, "Model-based pre-processing in Raman spectroscopy of biological samples," *J. Raman Spectrosc*, vol. 47, no. 6, pp. 643-650, 2016, doi: 10.1002/jrs.4886.

[21] P. H. C. Eilers, "A Perfect Smoother," *Anal. Chem*, vol. 75, no. 14, pp. 3631-3636, 2003, doi: 10.1021/ac034173t.

[22] I. G. Kolomnikov, A. M. Efremov, T. I. Tikhomirova, N. M. Sorokina, and Y. A. Zolotov, "Early stages in the history of gas chromatography," *JOURNAL OF CHROMATOGRAPHY A*, vol. 1537, pp. 109-117, 2018, doi: 10.1016/j.chroma.2018.01.006.

[23] D. A. Skoog, F. J. Holler, and S. R. Crouch, *Principles of instrumental analysis*, 7th edition ed. Boston, Mass: Cengage Learning, 2018.

[24] S. Instruments. "GC Fundamentals - What is Gas Chromatography." https://www.ssi.shimadzu.com/products/gas-chromatography/fundamental-guide-to-gas-chromatography/what-is-gas-chromatography.html#:~:text=Gas%20chromatography%20(GC)%20is%20an,can%20be%20separated%20and%20quantified (accessed 01.05.2022, 2022).

[25] S. Instruments. "Fundamental Guide to Gas Chromatography - Analysis Results." https://web.archive.org/web/20210421155339/https://www.ssi.shimadzu.com/products/gas-chromatography/fundamental-guide-to-gas-chromatography/analysis-results.html (accessed 01.05.2022, 2022).

[26] W. Zhang, Z. Yu, Q. Qian, Z. Zhang, and X. Wang, "Improving the pervaporation performance of the glutaraldehyde crosslinked chitosan membrane by simultaneously

changing its surface and bulk structure," *Journal of membrane science,* vol. 348, no. 1, pp. 213-223, 2010, doi: 10.1016/j.memsci.2009.11.003.

[27] C. Zhao *et al.,* "High performance composite membranes with a polycarbophil calcium transition layer for pervaporation dehydration of ethanol," *Journal of membrane science,* vol. 429, pp. 409-417, 2013, doi: 10.1016/j.memsci.2012.11.063.

[28] C. S. M. Pereira, V. M. T. M. Silva, S. P. Pinho, and A. E. Rodrigues, "Batch and continuous studies for ethyl lactate synthesis in a pervaporation membrane reactor," *Journal of membrane science,* vol. 361, no. 1, pp. 43-55, 2010, doi: 10.1016/j.memsci.2010.06.014.

[29] J. J. Jafar, P. M. Budd, and R. Hughes, "Enhancement of esterification reaction yield using zeolite A vapour permeation membrane," *Journal of membrane science,* vol. 199, no. 1, pp. 117-123, 2002, doi: 10.1016/S0376-7388(01)00683-4.

[30] N. Agoudjil, S. Kermadi, and A. Larbot, "Synthesis of inorganic membrane by sol–gel process," *Desalination,* vol. 223, no. 1, pp. 417-424, 2008, doi: 10.1016/j.desal.2007.01.187.

[31] R. Krupiczka and Z. Koszorz, "Activity-based model of the hybrid process of an esterification reaction coupled with pervaporation," *Separation and purification technology,* vol. 16, no. 1, pp. 55-59, 1999, doi: 10.1016/S1383-5866(98)00111-7.

[32] P. Delgado, M. T. Sanz, S. Beltrán, and L. A. Núñez, "Ethyl lactate production via esterification of lactic acid with ethanol combined with pervaporation," *Chemical engineering journal (Lausanne, Switzerland : 1996),* vol. 165, no. 2, pp. 693-700, 2010, doi: 10.1016/j.cej.2010.10.009.

[33] S. Assabumrungrat, J. Phongpatthanapanich, P. Praserthdam, T. Tagawa, and S. Goto, "Theoretical study on the synthesis of methyl acetate from methanol and acetic acid in pervaporation membrane reactors: effect of continuous-flow modes," *Chemical engineering journal (Lausanne, Switzerland : 1996),* vol. 95, no. 1, pp. 57-65, 2003, doi: 10.1016/S1385-8947(03)00084-6.

[34] Y. Zhu and H. Chen, "Pervaporation separation and pervaporation-esterification coupling using crosslinked PVA composite catalytic membranes on porous ceramic plate," *Journal of membrane science,* vol. 138, no. 1, pp. 123-134, 1998, doi: 10.1016/S0376-7388(97)00221-4.

[35] T. A. Peters, N. E. Benes, and J. T. F. Keurentjes, "Preparation of Amberlyst-coated pervaporation membranes and their application in the esterification of acetic acid and butanol," *Applied catalysis. A, General,* vol. 317, no. 1, pp. 113-119, 2007, doi: 10.1016/j.apcata.2006.10.006.

[36] B. Sarkar, S. Sridhar, K. Saravanan, and V. Kale, "Preparation of fatty acid methyl ester through temperature gradient driven pervaporation process," *Chemical engineering journal (Lausanne, Switzerland : 1996),* vol. 162, no. 2, pp. 609-615, 2010, doi: 10.1016/j.cej.2010.06.005.

[37] S.-M. Ahn, J.-W. Ha, J.-H. Kim, Y.-T. Lee, and S.-B. Lee, "Pervaporation of fluoroethanol/water and methacrylic acid/water mixtures through PVA composite membranes," *Journal of membrane science,* vol. 247, no. 1, pp. 51-57, 2005, doi: 10.1016/j.memsci.2004.09.005.

[38] J. M. Neel, Q. T. Nguyen, and H. Bruschke, "Composition membrane for separating water from fluids containing organic components by means of pervaporation," ed: Google Patents, 1994.

[39] P. M. Budd, N. M. P. S. Ricardo, J. J. Jafar, B. Stephenson, and R. Hughes, "Zeolite/Polyelectrolyte Multilayer Pervaporation Membranes for Enhanced Reaction Yield," *Ind. Eng. Chem. Res,* vol. 43, no. 8, pp. 1863-1867, 2004, doi: 10.1021/ie034142o.

[40] S. G. Adoor, L. S. Manjeshwar, S. D. Bhat, and T. M. Aminabhavi, "Aluminum-rich zeolite beta incorporated sodium alginate mixed matrix membranes for pervaporation dehydration and esterification of ethanol and acetic acid," *Journal of membrane science,* vol. 318, no. 1, pp. 233-246, 2008, doi: 10.1016/j.memsci.2008.02.043.

[41] N. Qureshi, M. M. Meagher, J. Huang, and R. W. Hutkins, "Acetone butanol ethanol (ABE) recovery by pervaporation using silicalite–silicone composite membrane from fed-batch reactor of Clostridium acetobutylicum," *Journal of membrane science,* vol. 187, no. 1, pp. 93-102, 2001, doi: 10.1016/S0376-7388(00)00667-0.

[42] T. Sano, S. Ejiri, K. Yamada, Y. Kawakami, and H. Yanagishita, "Separation of acetic acid-water mixtures by pervaporation through silicalite membrane," *Journal of Membrane Science,* vol. 123, no. 2, pp. 225-233, 1997, doi: 10.1016/s0376-7388(96)00224-4

[43] B. Smitha, D. Suhanya, S. Sridhar, and M. Ramakrishna, "Separation of organic–organic mixtures by pervaporation—a review," *Journal of Membrane Science,* vol. 241, no. 1, pp. 1-21, 2004, doi: 10.1016/j.memsci.2004.03.042.

[44] M. Krea, D. Roizard, N. Moulai-Mustefa, and D. Sacco, "Synthesis of polysiloxane-imide membranes — application to the extraction of organics from water mixtures," *Desalination,* vol. 163, no. 1-3, pp. 203-206, 2004, doi: 10.1016/S0011-9164(04)90190-7.

[45] M. Kaddour Djebbar, Q. T. Nguyen, R. Clément, and Y. Germain, "Pervaporation of aqueous ester solutions through hydrophobic poly(ether-block-amide) copolymer membranes," *Journal of membrane science,* vol. 146, no. 1, pp. 125-133, 1998, doi: 10.1016/S0376-7388(98)00090-8.

[46] M. T. Sanz and J. Gmehling, "Esterification of acetic acid with isopropanol coupled with pervaporation. Part I: Kinetics and pervaporation studies," *Chemical engineering journal (Lausanne, Switzerland : 1996),* vol. 123, no. 1-2, pp. 1-8, 2006, doi: 10.1016/j.cej.2006.06.006.

[47] L. Domingues, F. Recasens, and M. a. Larrayoz, "Studies of a pervaporation reactor: Kinetics and equilibrium shift in benzyl alcohol acetylation," *Chemical engineering science,* vol. 54, no. 10, pp. 1461-1465, 1999, doi: 10.1016/S0009-2509(99)00074-3.

[48] Z. Koszorz, N. Nemestothy, Z. Ziobrowski, K. Belafi-Bako, and R. Krupiczka, "Influence of pervaporation process parameters on enzymatic catalyst deactivation," *Desalination,* vol. 162, no. 1-3, pp. 307-313, 2004, doi: 10.1016/S0011-9164(04)00064-5.

[49] D. J. Benedict, S. J. Parulekar, and S.-P. Tsai, "Pervaporation-assisted esterification of lactic and succinic acids with downstream ester recovery," *Journal of membrane science,* vol. 281, no. 1, pp. 435-445, 2006, doi: 10.1016/j.memsci.2006.04.012.

[50] A. Hasanoğlu, Y. Salt, S. Keleşer, and S. Dinçer, "The esterification of acetic acid with ethanol in a pervaporation membrane reactor," *Desalination,* vol. 245, no. 1, pp. 662-669, 2009, doi: 10.1016/j.desal.2009.02.034.

[51] S. Korkmaz, Y. Salt, and S. Dincer, "Esterification of Acetic Acid and Isobutanol in a Pervaporation Membrane Reactor Using Different Membranes," *Ind. Eng. Chem. Res,* vol. 50, no. 20, pp. 11657-11666, 2011, doi: 10.1021/ie200086h.

[52] W. Zhang, W. Qing, N. Chen, Z. Ren, J. Chen, and W. Sun, "Enhancement of esterification conversion using novel composite catalytically active pervaporation membranes," *Journal of membrane science,* vol. 451, pp. 285-292, 2014, doi: 10.1016/j.memsci.2013.10.001.

[53] J. Ma, M. Zhang, L. Lu, X. Yin, J. Chen, and Z. Jiang, "Intensifying esterification reaction between lactic acid and ethanol by pervaporation dehydration using chitosan–TEOS hybrid membranes," *Chemical engineering journal (Lausanne, Switzerland : 1996),* vol. 155, no. 3, pp. 800-809, 2009, doi: 10.1016/j.cej.2009.07.044.

[54] L. Bagnell, K. Cavell, A. M. Hodges, A. W. Mau, and A. J. Seen, "The use of catalytically active pervaporation membranes in esterification reactions to simultaneously increase product yield, membrane permselectivity and flux," *Journal of Membrane Science,* vol. 85, no. 3, pp. 291-299, 1993, doi: 10.1016/0376-7388(93)85282-2.

[55] S. Korkmaz, Y. Salt, A. Hasanoglu, S. Ozkan, I. Salt, and S. Dincer, "Pervaporation membrane reactor study for the esterification of acetic acid and isobutanol using polydimethylsiloxane membrane," *Applied catalysis. A, General,* vol. 366, no. 1, pp. 102-107, 2009, doi: 10.1016/j.apcata.2009.06.037.

[56] P. Delgado, M. T. Sanz, and S. Beltrán, "Pervaporation of the quaternary mixture present during the esterification of lactic acid with ethanol," *Journal of membrane science,* vol. 332, no. 1, pp. 113-120, 2009, doi: 10.1016/j.memsci.2009.01.044.

[57] P. Delgado, M. T. Sanz, and S. Beltrán, "Pervaporation study for different binary mixtures in the esterification system of lactic acid with ethanol," *Separation and purification technology,* vol. 64, no. 1, pp. 78-87, 2008, doi: 10.1016/j.seppur.2008.08.002.

[58] E. Sert and F. S. Atalay, "n-Butyl acrylate production by esterification of acrylic acid with n-butanol combined with pervaporation," *Chemical engineering and processing,* vol. 81, pp. 41-47, 2014, doi: 10.1016/j.cep.2014.04.010.

[59] P. Cote, "Mass transfer limitations in pervaporation for water and waste water treatment," in *Proceeding of Third International Conference on Pervaporation Processes*, 1988, pp. 449-462.

[60] K. C. S. Figueiredo, V. M. M. Salim, and C. P. Borges, "Ethyl oleate production by means of pervaporation-assisted esterification using heterogeneous catalysis," *Brazilian journal of chemical engineering,* vol. 27, no. 4, pp. 609-617, 2010, doi: 10.1590/S0104-66322010000400013.

[61] B.-G. Park and T. T. Tsotsis, "Models and experiments with pervaporation membrane reactors integrated with an adsorbent system," *Chemical engineering and processing,* vol. 43, no. 9, pp. 1171-1180, 2004, doi: 10.1016/j.cep.2003.10.008.

[62] Y. Zhu, R. G. Minet, and T. T. Tsotsis, "A continuous pervaporation membrane reactor for the study of esterification reactions using a composite polymeric/ceramic membrane," *Chemical engineering science*, vol. 51, no. 17, pp. 4103-4113, 1996, doi: 10.1016/0009-2509(96)00252-7.

[63] Y. Zou, Z. Tong, K. Liu, and X. Feng, "Modeling of Esterification in a Batch Reactor Coupled with Pervaporation for Production of n-Butyl Acetate," *Chinese journal of catalysis*, vol. 31, no. 8, pp. 999-1005, 2010, doi: 10.1016/S1872-2067(10)60100-3.

[64] H. Zhou, Y. Li, G. Zhu, J. Liu, L. Lin, and W. Yang, "Microwave synthesis of a&b-oriented zeolite T membranes and their application in pervaporation-assisted esterification," *Chinese journal of catalysis*, vol. 29, no. 7, pp. 592-594, 2008, doi: 10.1016/S1872-2067(08)60059-5.

[65] K. Tanaka, R. Yoshikawa, C. Ying, H. Kita, and K.-i. Okamoto, "Application of zeolite membranes to esterification reactions," *Catalysis today*, vol. 67, no. 1, pp. 121-125, 2001, doi: 10.1016/S0920-5861(01)00271-1.

[66] E. Ameri, A. Moheb, and S. Roodpeyma, "Vapor-permeation-aided esterification of isopropanol/propionic acid using NaA and PERVAP ® 2201 membranes," *Chemical engineering journal (Lausanne, Switzerland : 1996)*, vol. 162, no. 1, pp. 355-363, 2010, doi: 10.1016/j.cej.2010.05.018.

[67] A. V. Penkova, G. A. Polotskaya, and A. M. Toikka, "Separation of acetic acid–methanol–methyl acetate–water reactive mixture," *Chemical engineering science*, vol. 101, pp. 586-592, 2013, doi: 10.1016/j.ces.2013.05.055.

[68] S. Khajavi, J. C. Jansen, and F. Kapteijn, "Application of a sodalite membrane reactor in esterification—Coupling reaction and separation," *Catalysis today*, vol. 156, no. 3, pp. 132-139, 2010, doi: 10.1016/j.cattod.2010.02.042.

[69] M. Pilar Bernal, J. n. Coronas, M. Menéndez, and J. Santamaría, "Coupling of reaction and separation at the microscopic level: esterification processes in a H-ZSM-5 membrane reactor," *Chemical engineering science*, vol. 57, no. 9, pp. 1557-1562, 2002, doi: 10.1016/S0009-2509(02)00030-1.

[70] A. Penkova, G. Polotskaya, and A. Toikka, "Pervaporation composite membranes for ethyl acetate production," *Chemical engineering and processing*, vol. 87, pp. 81-87, 2015, doi: 10.1016/j.cep.2014.11.015.

[71] F. Xianshe and R. Y. M. Huang, "Studies of a membrane reactor: Esterification facilitated by pervaporation," *Chemical engineering science*, vol. 51, no. 20, pp. 4673-4679, 1996, doi: 10.1016/0009-2509(96)00316-8.

[72] K. Wasewar, S. Patidar, and V. K. Agarwal, "Esterification of lactic acid with ethanol in a pervaporation reactor: modeling and performance study," *Desalination*, vol. 243, no. 1, pp. 305-313, 2009, doi: 10.1016/j.desal.2008.04.030.

[73] A. P. Rathod, K. L. Wasewar, and S. S. Sonawane, "Intensification of Esterification Reaction of Lactic Acid with Iso-propanol using Pervaporation Reactor," *Procedia Engineering*, vol. 51, pp. 456-460, 2013, doi: 10.1016/j.proeng.2013.01.064.

[74] A. P. Rathod, K. L. Wasewar, and S. S. Sonawane, "Enhancement of Esterification Reaction by Pervaporation Reactor: An Intensifying Approach," *Procedia Engineering*, vol. 51, pp. 330-334, 2013, doi: 10.1016/j.proeng.2013.01.045.

[75] G. S. Gokavi, M. G. Mali, U. V. Desai, and T. M. Aminabhavi, "Highly Water Selective Mixed Matrix Blend Membranes of Poly(Vinyl Alcohol)–Poly(Vinyl Pyrolidone) Incarporating Phosphomolybdic Acid for Application in Pervaporation Assisted Esterification of Acetic Acid with Ethanol," *Procedia engineering,* vol. 44, pp. 845-846, 2012, doi: 10.1016/j.proeng.2012.08.594.

[76] M. David, "Pervaporation-esterification coupling: part I. Basic kinetic model," *Chem. Eng. Res. Des.*, vol. 69, pp. 335-340, 1991.

[77] L. Xuehui and W. Lefu, "Kinetic model for an esterification process coupled by pervaporation," *Journal of membrane science,* vol. 186, no. 1, pp. 19-24, 2001, doi: 10.1016/S0376-7388(00)00653-0.

[78] Q. Liu, Z. Zhang, and H. Chen, "Study on the coupling of esterification with pervaporation," *Journal of membrane science,* vol. 182, no. 1, pp. 173-181, 2001, doi: 10.1016/S0376-7388(00)00568-8.

[79] F. Xianshe and R. Y. M. Huang, "Estimation of activation energy for permeation in pervaporation processes," *Journal of membrane science,* vol. 118, no. 1, pp. 127-131, 1996, doi: 10.1016/0376-7388(96)00096-8.

[80] A. Grob and A. Heintz, "Sorption isotherms of aromatic compounds in organophilic polymer membranes used in pervaporation," *Journal of solution chemistry*, vol. 28, no. 10, pp. 1159-1174, 1999, doi: 10.1023/a:1021755709161.

[81] M. C. Burshe, S. B. Sawant, and V. G. Pangarkar, "Dehydration of glycerine-water mixtures by pervaporation," *Journal of the American Oil Chemists' Society,* vol. 76, no. 2, pp. 209-214, 1999, doi: 10.1007/s11746-999-0220-2.

[82] K.-H. Song, K.-R. Lee, and J.-M. Rim, "Pervaporation of esters with hydrophobic membrane," *The Korean journal of chemical engineering,* vol. 21, no. 3, pp. 693-698, 2004, doi: 10.1007/BF02705507.

[83] W. F. Guo, T.-S. Chung, and T. Matsuura, "Pervaporation study on the dehydration of aqueous butanol solutions: a comparison of flux vs. permeance, separation factor vs. selectivity," *Journal of membrane science,* vol. 245, no. 1, pp. 199-210, 2004, doi: 10.1016/j.memsci.2004.07.025.

[84] A. Hasanoğlu, Y. Salt, S. Keleşer, S. Özkan, and S. Dinçer, "Pervaporation separation of organics from multicomponent aqueous mixtures," *Chemical engineering and processing,* vol. 46, no. 4, pp. 300-306, 2007, doi: 10.1016/j.cep.2006.06.010.

[85] C. J. Knill and J. F. Kennedy, "Polymer handbook (4th Edition): J. Brandrup, E.H. Immergut, E.A. Grulke (Eds.); Wiley, New York, 1999, xiii+2288 pages, ISBN 0-471-16628-6 (£226-00)," vol. 46, ed: Elsevier Ltd, 2001, pp. 295-295.

[86] M. Mulder, *Thermodynamic principles of pervaporation* (Pervaporation membrane separation processes. Chapter 4). Amsterdam, The Netherlands: Elsevier, 1991, pp. 225-250.

[87] HYDROSCAND. "ARMERT PVC SLANGE (NM KVALITET)." https://www.hydroscand.no/hydropedia/slanger/1422-30 (accessed 19th April, 2022).

[88] W. A. Noyes and R. R. Warfel, "The Boiling-Point Curve for Mixtures of Ethyl Alcohol and Water," *J. Am. Chem. Soc,* vol. 23, no. 7, pp. 463-468, 1901, doi: 10.1021/ja02033a004.

[89] E. ToolBox. "Water - Boiling Points at Vacuum Pressure." https://www.engineeringtoolbox.com/water-evacuation-pressure-temperature-d_1686.html (accessed 15th May, 2022).

[90] E. ToolBox. "Ice and Water - Melting Points vs. Pressure." https://www.engineeringtoolbox.com/water-melting-temperature-point-pressure-d_2005.html (accessed 15th May, 2022).

[91] W. Yave, "Separation performance of improved PERVAPTM membrane and its dependence on operating conditions," *Journal of membrane science and research*, vol. 5, no. 3, pp. 216-221, 2019, doi: 10.22079/JMSR.2018.88186.1198.

Appendices

Appendix A: The esterification experiments plan

Experiment	Membrane	Initial volume (ml)	Catalyst loading (g/l)
1	PERVAP™ 4100	600	4
2		400	4
3		500	4
4		500	2
5		500	8
6	PERVAP™ 4101	600	4
7		400	4
8		500	4
9		500	2
10		500	8
11	Without pervaporation	500	2
12		500	4
13		500	8

Appendix B: Microsoft Excel spread sheet used to find composition of experiment sample.

In here in-built Goal Seek function was used to find the ethanol composition of the sample.

Tested samples	Ethanol				
	w/w %	Intensity obtained from test	Wavelength	Intensity calculated	Difference between actual and calculated intensities
Eth 0 Eth Wat Cal Curve - Probe 1 Experiment 2022-04-05 17-21	0	1.28E-04	879	0.0001	
Eth 5 Eth Wat Cal Curve Probe 1 Experiment 2022-04-05 17-37	5.0536	9.61E-02	879	0.0845	
Eth 10 Eth Wat Cal Curve Probe 1 Experiment 2022-04-05 17-49	10.0518	1.93E-01	879	0.1680	
Eth 15 Eth Wat Cal Curve Probe 1 Experiment 2022-04-05 17-49	15.1075	2.87E-01	879	0.2524	
Eth 20 Eth Wat Cal Curve Probe 1 Experiment 2022-04-05 18-36	19.7775	3.72E-01	879	0.3304	
Eth 25 Eth Wat Cal Curve Probe 1 Experiment 2022-04-05 18-46	25.0315	4.69E-01	879	0.4182	
Eth 50 Eth Wat Cal Curve Probe 1 Experiment 2022-04-05 18-54	50.0597	8.56E-01	881	0.8361	
Eth 75 Eth Wat Cal Curve Probe 1 Experiment 2022-04-05 19-02	75.0332	1.27E+00	882	1.2532	
Eth 85 Eth Wat Cal Curve Probe 1 Experiment 2022-04-05 19-26	84.2778	1.41E+00	882	1.4076	
Eth 90 Eth Wat Cal Curve Probe 1 Experiment 2022-04-05 19-28	90.0004	1.50E+00	883	1.5031	
Eth 95 Eth Wat Cal Curve Probe 1 Experiment 2022-04-05 19-34	95.0334	1.57E+00	883	1.5872	
Eth 100 Eth Wat Cal Curve Probe 1 Experiment 2022-04-05 19-40	99.9000	1.63E+00	883	1.6685	
Ex8 Reac0 Probe 1 Experiment 2022-04-20 17-52	6.29E+01	1.05E+00	882	1.0506	2.34E-05
Ex8 Reac1 Probe 1 Experiment 2022-04-20 17-57	6.48E+01	1.08E+00	882	1.0818	2.80E-05
Ex8 Reac2 Probe 1 Experiment 2022-04-20 18-03	6.63E+01	1.11E+00	882	1.1077	3.03E-05
Ex8 Reac3 Probe 1 Experiment 2022-04-20 18-08	7.03E+01	1.17E+00	882	1.1749	3.13E-05
Ex8 Reac4 Probe 1 Experiment 2022-04-20 18-14	7.53E+01	1.26E+00	882	1.2576	2.20E-05
Ex8 Reac5 Probe 1 Experiment 2022-04-20 18-17	7.92E+01	1.32E+00	882	1.3223	6.71E-06